

Seasonal and Interannual Variability of Pigment Concentrations Across a California Current Frontal Zone

A. C. THOMAS AND P. T. STRUB

College of Oceanography, Oregon State University, Corvallis

Previously published physical and biological data document a zonally oriented frontal region within the California Current system separating colder and more eutrophic water north of $\approx 33^\circ\text{N}$ from warmer, more stratified, and oligotrophic water farther to the south. Satellite images of phytoplankton pigment from the coastal zone color scanner from 1979–1983 and 1986 are used to examine the seasonal and interannual variability of both the latitudinal position of this front and the pigment concentrations associated with it. Many temporal and spatial characteristics of the pigment structure are repeated in different years, and a general seasonal cycle is described. Variations in the frontal structure are controlled primarily by changes in pigment concentration north of the front. Seasonality is minimum south of the front where concentrations remain low ($<0.5\text{ mg m}^{-3}$) throughout the spring, summer, and fall. The frontal gradient is typically strongest from late March until early June when higher concentrations ($>2.0\text{ mg m}^{-3}$) are present north of the front. Lower pigment concentrations within the sampled region ($0.5\text{--}1.0\text{ mg m}^{-3}$) north of the front in mid-late summer (June–August), resulting from a seasonal shift in the cross-shelf distribution of pigment, reduce and often eliminate the pigment gradient forming the front. Concentrations greater than 1.0 mg m^{-3} typically extend 150–250 km farther offshore in spring (April) than in summer (June–July). Superimposed on this general seasonality is strong interannual variability in the magnitude of the frontal gradient, its latitudinal position, and the seasonal development of higher biomass in regions north of the front. Pigment concentrations during the El Niño year of 1983 are distinctly lower than those of other years. The patterns evident in the satellite data are compared with available in situ measured hydrographic data and nutrient and phytoplankton concentrations. A comparison of the seasonal and interannual variability of these patterns to surface wind shows little direct relation between frontal strength or position and wind forcing.

1. INTRODUCTION

Characteristics of the flow within the California Current system (CCS) are highly variable in both space and time [Hickey, 1979]. Large-scale variability and forcing of this eastern boundary current is discussed by Lynn and Simpson [1987] and Strub *et al.* [1987a]. In general, the flow of the CCS in regions away from the shelf and shelf break is equatorward throughout the year. At a latitude of $\approx 32^\circ\text{N}$, however, this flow makes an eastward turn toward the coast. The core of the CCS occurs 300 to 400 km offshore north of this latitude but is found within 200 km of the coast off Baja California [Lynn and Simpson, 1987]. This shoreward flow forms the southern portion of the cyclonic flow in the Southern California Bight (SCB) and feeds the northward flow along the coast off central California described by Chelton *et al.*, 1988; Strub *et al.*, 1987a; and Wickham *et al.*, 1987. The rest of the CCS continues equatorward along the Baja coast [Wyllie, 1966]. This onshore flow is evident in hydrographic data [Wyllie, 1966; Roesler and Chelton, 1987; Simpson *et al.*, 1987] and in drifter data [Reid *et al.*, 1963]. More recently, Niler *et al.* [1989] described the three-dimensional structure of this feature, presenting evidence for significant upwelling within its core. Pares-Sierra and O'Brien [1989] demonstrate that this flow pattern is a stable feature of a nonlinear,

reduced gravity model forced by wind stress and wind stress curl. The absence of any topographic effects in their model indicates that this feature is not a result of bottom topography. The latitudinal variability in the position of this eastward flow produces a zonal maximum in the long-term (≈ 30 years) variability of dynamic height over southern portions of the CCS [Lynn and Simpson, 1987].

This eastward flow forms a zonally oriented frontal region within the CCS which separates warmer and more oligotrophic water from more eutrophic water found both to the north and farther south off Baja [Peláez and McGowan, 1986; Strub *et al.*, 1990]. The frontal zone is the southern boundary of the extensive offshore region of higher biomass associated with the upwelling and cross-shelf transport characteristic of northern and central California during the summer. North of the front, physical forcing within the CCS is dominated by strong seasonality in upwelling, offshore transport, and wind mixing. South of the front, seasonality is much weaker, and upwelling winds occur throughout the year [Strub *et al.*, 1987a]. The seasonal development of phytoplankton biomass to the north of the front can therefore be expected to contrast strongly with that south of the front.

The spatial and temporal characteristics of this frontal zone have biological implications at most trophic levels of the planktonic community of the CCS. Peláez and Guan [1982] show a strong, latitudinally oriented, frontal zone in coastal zone color scanner (CZCS) satellite images of phytoplankton pigment concentration of this region for the summer of 1981, with higher concentrations restricted to regions north of the frontal zone. Peláez and McGowan [1986] use a series of individual CZCS images from

Copyright 1990 by the American Geophysical Union

Paper number 90JC01181.
0148-0227/90/90JC-01181\$05.00

1981 and 1982 to illustrate a seasonal change in the position of the frontal zone. During these years the frontal zone in their images moves south in spring and summer and reaches its southernmost position in August or September. The cross-frontal pigment gradient weakens in late summer and then moves northward in fall and winter. *Peláez and McGowan* present coincident CZCS and hydrographic data that support the hypothesis that low pigment concentrations south of the front are due to the onshore flow of oligotrophic offshore water in this semipermanent meander of the CCS. *Haury* [1984] shows decreases in the concentration of zooplankton species commonly associated with CCS water in meridional transects from north to south across this region which are coincident with an increase in pycnocline and nutricline depth shown by *Simpson* [1984a]. Maps of euphausiid species distribution presented by *Brinton* [1967] indicate that this frontal region is an important faunal boundary. *Fiedler* [1984] shows that the northern and offshore extent of anchovy spawning in this region in 1980 is limited by a frontal region of colder water advected southward from the Point Conception area. Interannual variability of the albacore tuna catch in the SCB is also thought to be related to the strength and position of this frontal zone [*M. Laurs, personal communication, 1989*].

A systematic analysis of the mesoscale seasonal and interannual variability of phytoplankton distributions in this region has not been made. In this study we utilize CZCS imagery from 6 years to contrast temporal characteristics of the pigment concentration to the north of the front with those south of the front and to examine the latitudinal variability of the frontal zone. Processing of the satellite imagery is discussed in section 2. The data are presented in section 3 using both time series of pigment concentrations and specific examples of recurrent features identified as a seasonal pattern. In section 4, spatial patterns and seasonality evident in the imagery are discussed in relation to meridional transects of physical, chemical, and biological data available from California Cooperative Oceanic Fisheries Investigations (CalCOFI) cruises and time series of wind stress and mixing, contrasting the physical forcing in northern and southern portions of the study area. A summary and conclusions are presented in section 5.

2. DATA AND METHODS

The CZCS images used in this study were recorded at the Scripps Satellite Oceanography Facility and processed at the Jet Propulsion Laboratory to form the West Coast time series (WCTS) under the direction of M. Abbott (details of the processing are given by *Strub et al.* [1990]). Initial calculations made use of the entire WCTS, which covers the period from mid-1979 to mid-1986. A severe lack of data in 1984 and 1985, due to difficulties with the sensor, prevented the formation of a meaningful time series in these years, and they were not included in this analysis. The final time series presented here covers the period from mid-July 1979 to December 1983 and from January to mid-June 1986.

Accuracy of the CZCS pigment measurements is estimated to be \log [Chlorophyll] ± 0.5 by *Gordon et al.* [1980, 1983] for summer data. *Smith et al.* [1988] showed the similarity between the CZCS data and ship data from the southern California coast to be $\pm 40\%$ for pigment concentrations between 0.05 and 10.0 mg m⁻³. Regres-

sion of log transformed WCTS satellite pigment on ship chlorophyll [*Abbott and Zion, 1987*] results in an r^2 of 0.8 and a slope of 1.0 for summer data off northern California. The atmospheric correction algorithm used to process the WCTS is known to overestimate pigment concentrations at the large solar zenith angles present during winter at higher latitudes. Examination of pigment time series (presented in section 3) identified winter periods of high pigment concentration (often >3.0 mg m⁻³) in each year. These concentrations are more than 3 times higher than those found during winter CalCOFI cruises to the same region in 1984 and 1985 [*Scripps Institution of Oceanography (SIO), 1984a, b, 1985b*]. The winter period over which the data are not valid could be subjectively identified within the time series in a manner consistent from year to year (discussed in section 4). In general terms, winter data in the WCTS from the months November, December, January, and February in each year appear to be affected by the image processing error and will not be discussed in this paper. A detailed discussion of known problems of the WCTS data set is presented by *Strub et al.* [1990].

The WCTS data used in this study consist of the mosaic images covering the west coast from $\approx 22^\circ\text{N}$ to 55°N at a spatial resolution of ≈ 14.3 pixels per degree. Further temporal and spatial averaging is used to reduce gaps in the image time series. Although this averaging decreases both the spatial and temporal resolution of the satellite data, it produces a more uniform time series than that of individual images. The averaging is an effective compromise between the quantitative utilization of as much of the archived satellite data set as possible, estimating position and variability of the desired oceanographic features, and filling gaps caused by clouds and missing data. Ten-day composites of each pixel are formed using all images in the first 360 days of each year. Each of the composites formed in this study can be considered statistically independent, since the temporal separation of the data within them (average of 10 days), is considerably longer than previous estimates of the time scales of decorrelation of surface patterns in color and infrared satellite imagery. *Thomas and Emery* [1988] estimate a decorrelation time scale of 2–3 days for the continental shelf region off southern British Columbia, and *Kelly* [1983] estimates 4–5 days for the Coastal Ocean Dynamics Experiment (CODE) region off central California. *Denman and Abbott* [1988] show that features at length scales between 50 and 150 km become decorrelated at time scales of 7 to 10 days in the CCS off British Columbia and Washington.

The 10-day composite images are then subsampled by longitudinally averaging across a 100-km-wide, latitudinally oriented transect running from $\approx 38^\circ\text{N}$ to $\approx 30^\circ\text{N}$ (Figure 1). Latitudinal resolution along this meridional transect is equal to the pixel resolution of the mosaic images (≈ 8 km). This procedure results in 120 potential data points per transect for each of the 36 time periods in each year (except 1979 and 1986, for which only 6 months of data are available). A second subset of the data (a zonal transect, see Figure 1) is formed to allow a comparison of the spring and summer cross-shelf distribution of pigment concentration in the northern portion of the study area. The mean cross-shelf pigment distribution within the region shown in Figure 1 is calculated by latitudinally averaging pixels from south to north, ($\approx 35^\circ\text{N}$ to 38°N , 45 pixels) in

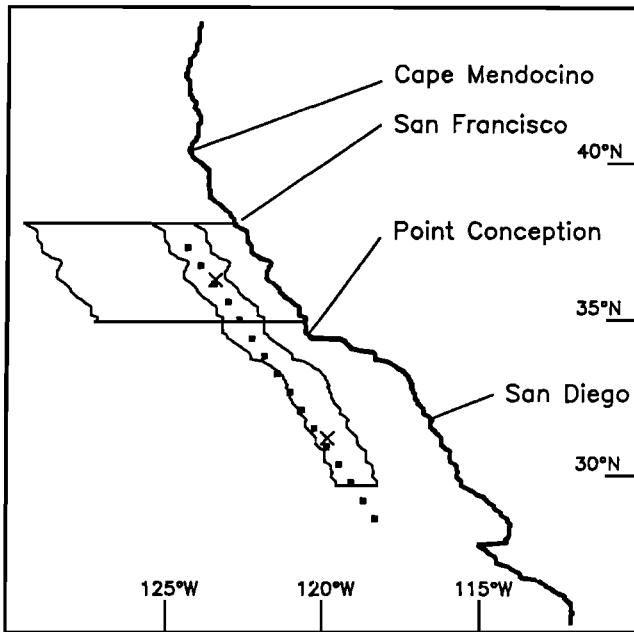


Fig. 1. A coastal outline of the study area showing major geographic points. The 100 km wide meridional transect within which data are zonally averaged from each of the 10-day composite images is shown, as are the locations of CalCOFI station 70 from each of the CalCOFI lines from which in situ data are reported. The latitudinal and offshore extent of the region over which an average cross-shelf transect is formed is also shown (extending offshore north of 35°N). The two grid points from which LFM wind values are used to characterize wind forcing over the northern and southern portions of the transect are shown by crosses.

three consecutive 10-day composites in spring (April–May) and summer (June–July) of each year (except 1979). These three mean transects are then averaged together to form an overall mean spring and summer cross-shelf pigment distribution. Each of these transects has 95 spatial points, extending ≈ 760 km offshore.

Despite the spatial and temporal averaging, gaps due to clouds and lack of data persist in the time series. At each spatial point, these gaps are filled by optimal interpolation in time. The gaps account for 25.1% of the total number of points making up the space and time series of the meridional transect (120 space points and 181 time points). The nature of these gaps is such that missing data tend to co-occur temporally at the spatial points, and gaps of more than three consecutive (10 day) periods are rare. Temporal averaging of the three cross-shelf transects in spring and summer of each year eliminated all missing data points in each period.

In situ measurements of density structure, nitracline depth, and nutrient and chlorophyll concentration are taken from available CalCOFI data reports. Daily wind velocities at grid points covering the study area are available from the limited-area fine mesh (LFM) data set from the National Meteorological Center.

3. RESULTS

Image-derived pigment concentrations along the meridional transect are plotted as contours in time and latitude

in Figure 2 for the periods of available data. These data show the seasonal development of pigment concentrations from 38.1°N to 29.7°N in each year, identifying times and latitudes when strong gradients develop and a frontal zone is present. In the following presentation we take concentrations less than 0.5 mg m^{-3} to be indicative of oligotrophic water of southern and/or offshore origin and the gradient between this and concentrations greater than 1.0 mg m^{-3} to be the primary signature of the frontal zone. An examination of contours less than 0.5 mg m^{-3} showed this to be a consistent representation of the frontal zone.

Concentrations appear relatively high (often $>3.0 \text{ mg m}^{-3}$) in the winter months (\approx November–February) of each year, most consistently north of $\approx 32^\circ\text{N}$. The extent to which this winter seasonal maximum in the WCTS data represents actual pigment concentration within the water column is unknown. The atmospheric correction algorithm used to process the WCTS produces artificially high values at the large solar zenith angles present in winter. Both the late spring increase and the late fall decrease in pigment concentration, however, run counter to the trend imposed by algorithm error and are probably not an artifact of the data processing. This argues that although the actual concentrations within these features might be influenced by algorithm problems, the observed trends and associated patterns between the spring increase and the fall decrease are at least qualitatively correct. If the spring increase and the fall decrease in concentration are accepted as real, the periods of uniform low concentration immediately after and before the winter maxima can be believed. This is supported by the previously mentioned CalCOFI data from 1984 and 1985. In this paper, we accept as valid those data in each year between the spring and fall periods of uniform low pigment concentration within the transect evident in Figure 2. The winter data are presented in Figure 2 only for completeness; the time periods within which the data are considered valid are indicated on each time series.

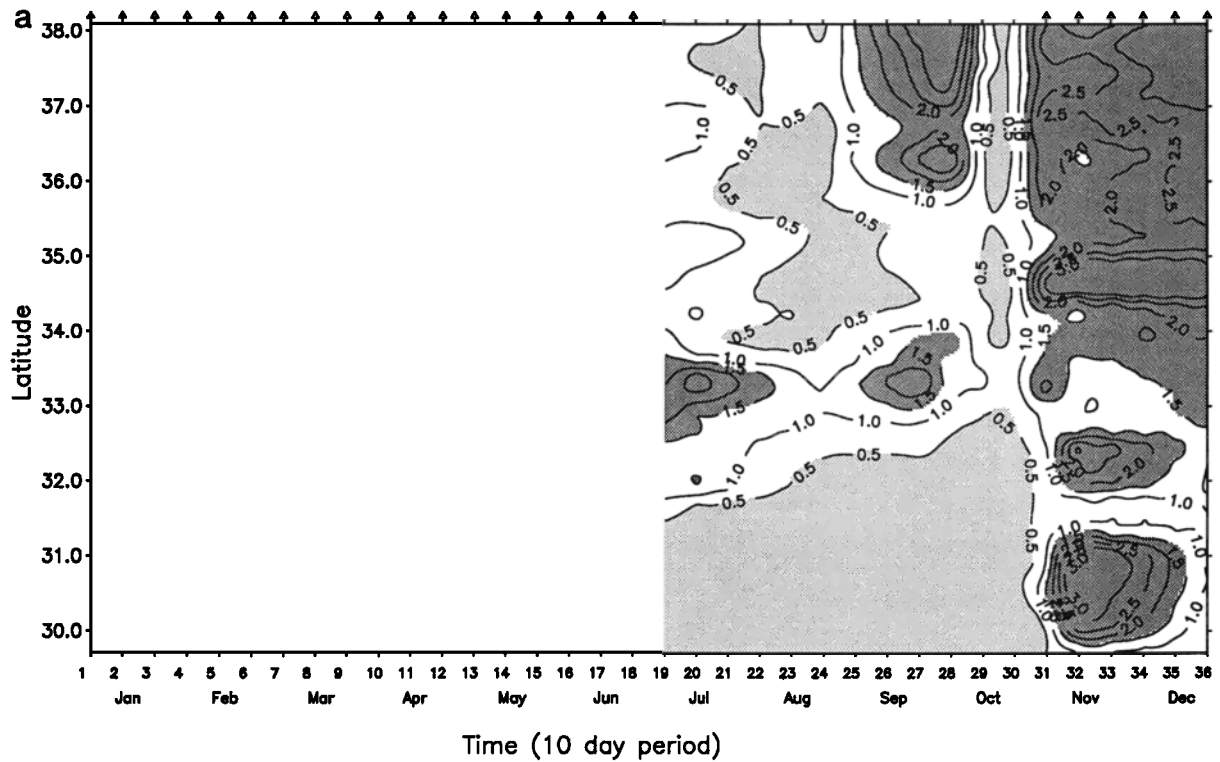
3.1. The Seasonal Cycle

Interannual comparison of the data in Figure 2 indicates that a number of features of the seasonal development of pigment concentration along the transect recur in different years and a generalized seasonal cycle is evident. The principal features of this cycle are presented below and illustrated in Figure 3 as individual transects using specific (10-day average) periods from 1981 as an example.

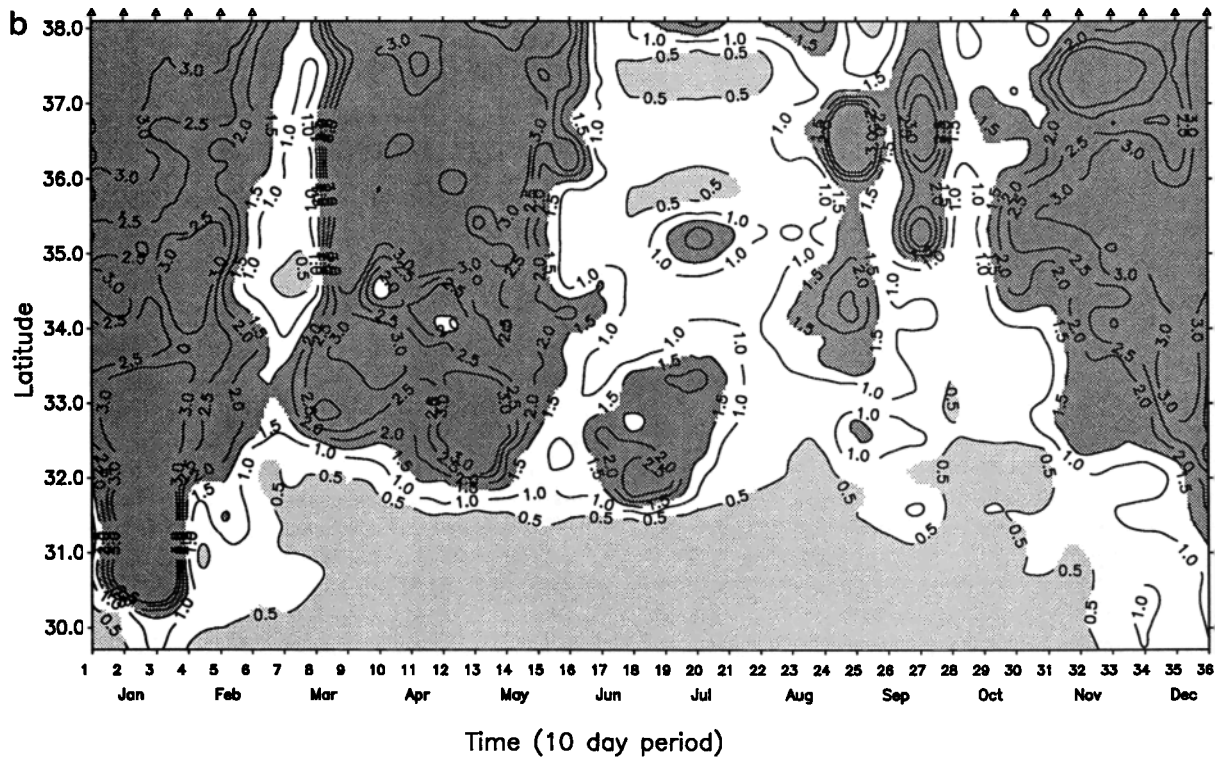
1. Low pigment concentrations (often $<0.5 \text{ mg m}^{-3}$) are present over the entire latitudinal range of the study area in the early spring (sometime in March or April).

2. Concentrations in the southern portion of the transect (south of $\approx 32^\circ\text{N}$) remain less than 0.5 mg m^{-3} from spring, throughout the summer and into the fall. There is, however, considerable seasonal and interannual variability in the location of the northern limit of this oligotrophic water.

3. North of $\approx 32^\circ\text{N}$, pigment concentrations during the year show a large degree of seasonal variability. In general, a sudden (often within 10 days) increase in concentration takes place in the late spring. This establishes a strong frontal gradient during the early portion of the summer separating oligotrophic water ($<0.5 \text{ mg m}^{-3}$) from higher pigment concentrations to the north ($>2.0 \text{ mg m}^{-3}$).

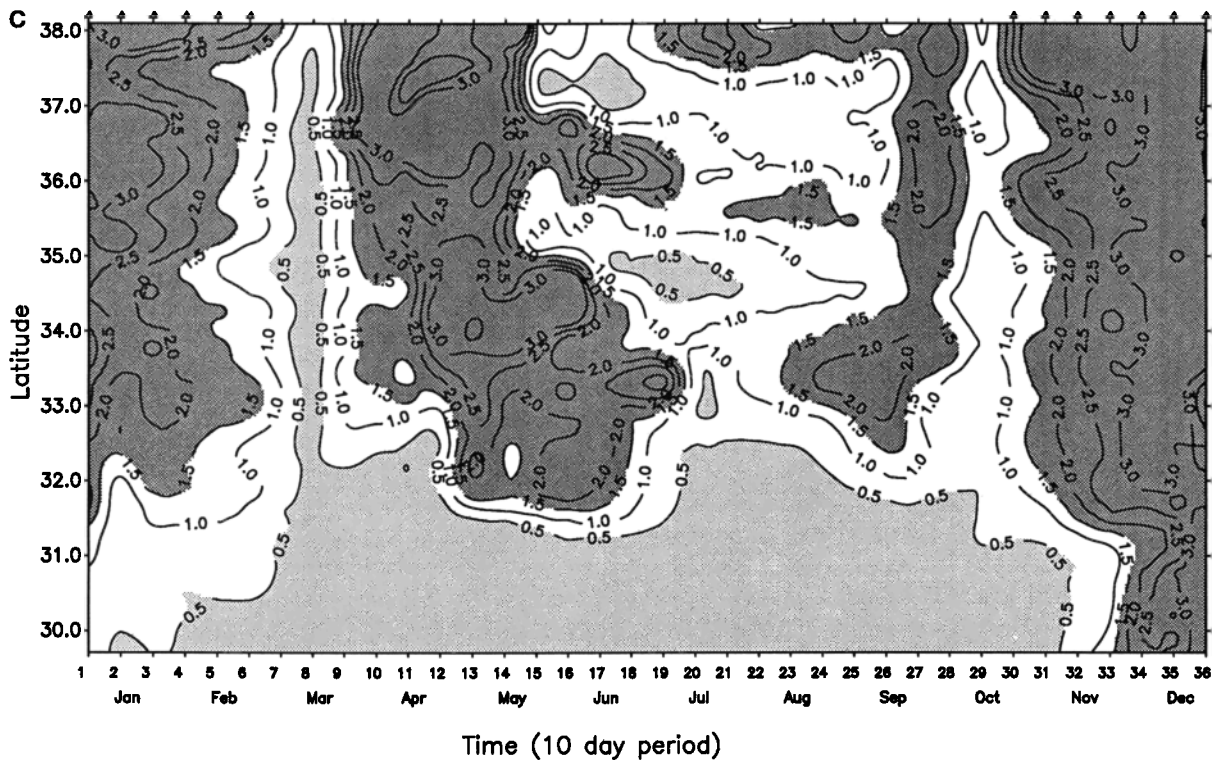


CZCS [CHL] contours in Time and Latitude for 1979

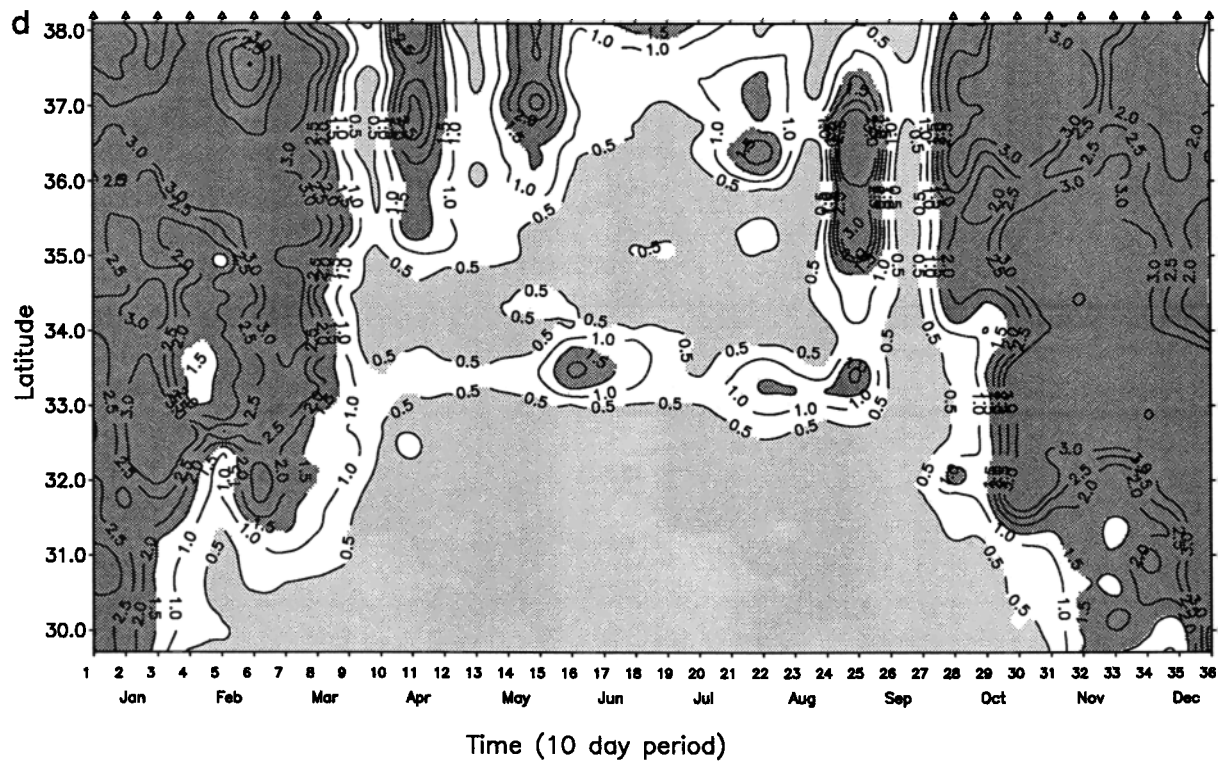


CZCS [CHL] contours in Time and Latitude for 1980

Fig. 2. Contours of phytoplankton pigment concentration in time and latitude from the meridional transect in Figure 1 for (a) 1979, (b) 1980, (c) 1981, (d) 1982, (e) 1983, and (f) 1986. Contours of concentrations greater than 3.0 mg m^{-3} are not shown for clarity. Each year (except 1979 and 1986; see text) comprises 36 meridional transects in time, each representing a 10-day image composite, and 120 alongshore measurements ($\approx 8 \text{ km}$ resolution) representing the mean concentration at each latitude over the width of the transect. Winter periods over which the data are suspect on account of algorithm error and periods in 1979 and 1986 of missing data are shown at the top of each plot as open triangles.

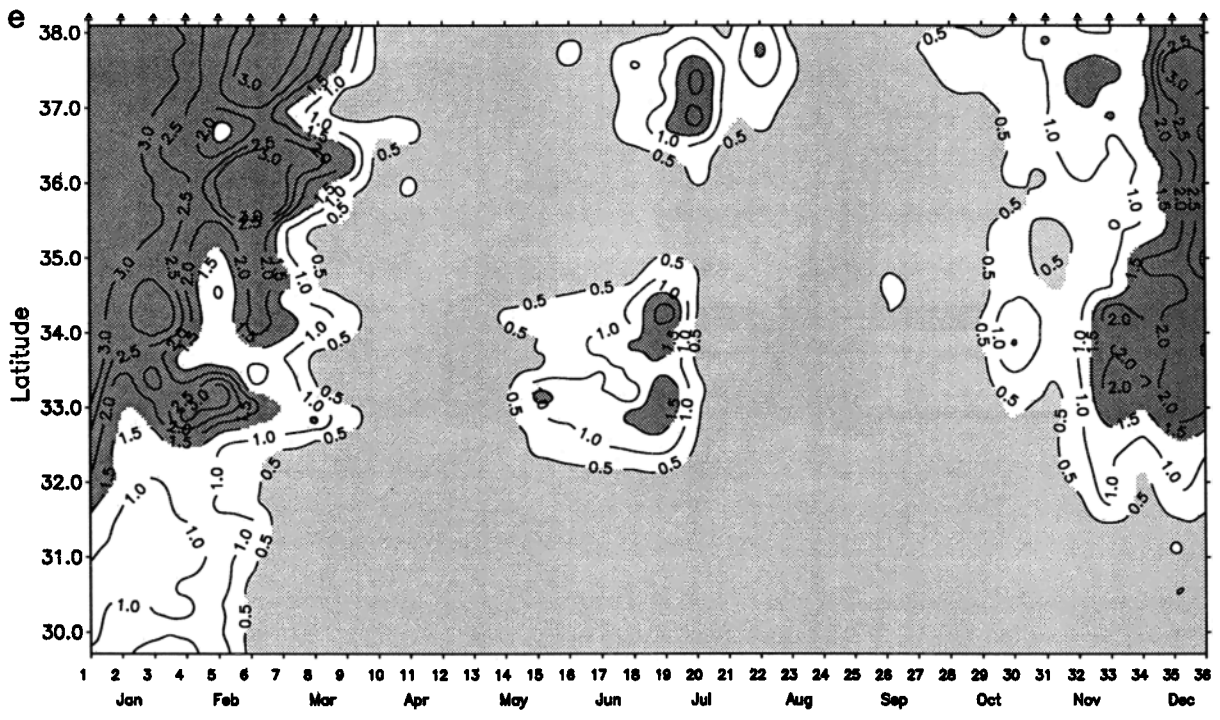


CZCS [CHL] contours in Time and Latitude for 1981

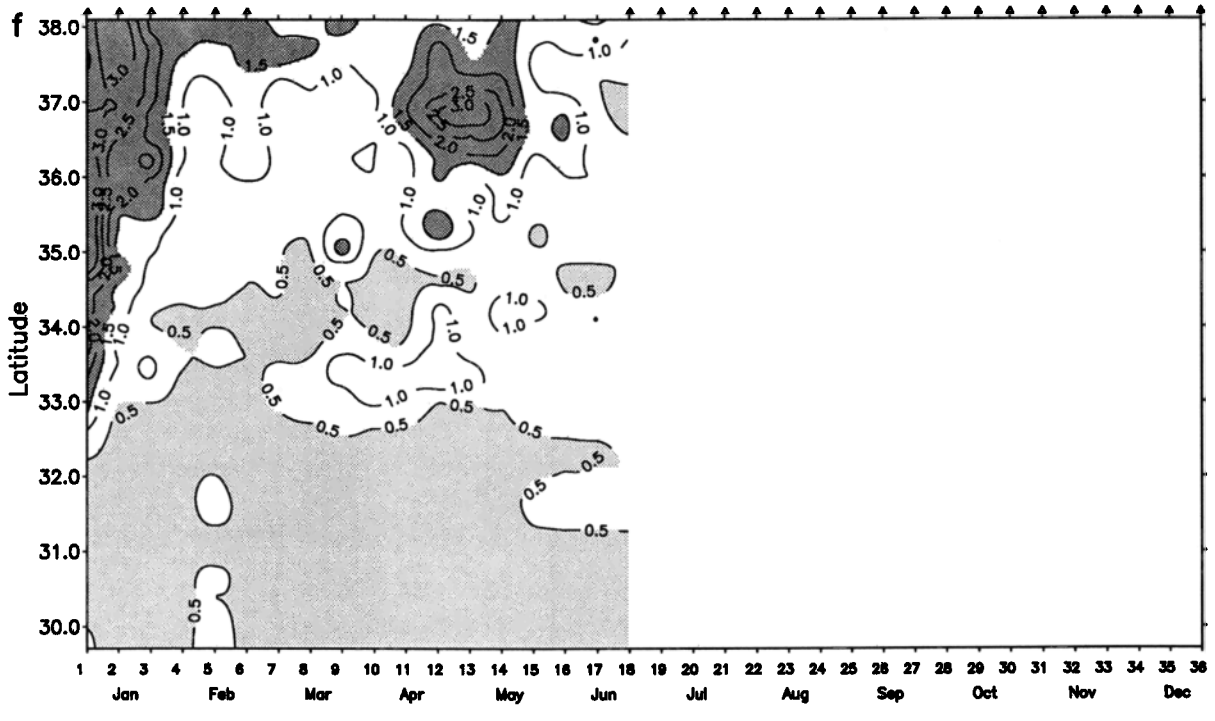


CZCS [CHL] contours in Time and Latitude for 1982

Fig. 2. (continued)



Time (10 day period)
CZCS [CHL] contours in Time and Latitude for 1983



Time (10 day period)
CZCS [CHL] contours in Time and Latitude for 1986

Fig. 2. (continued)

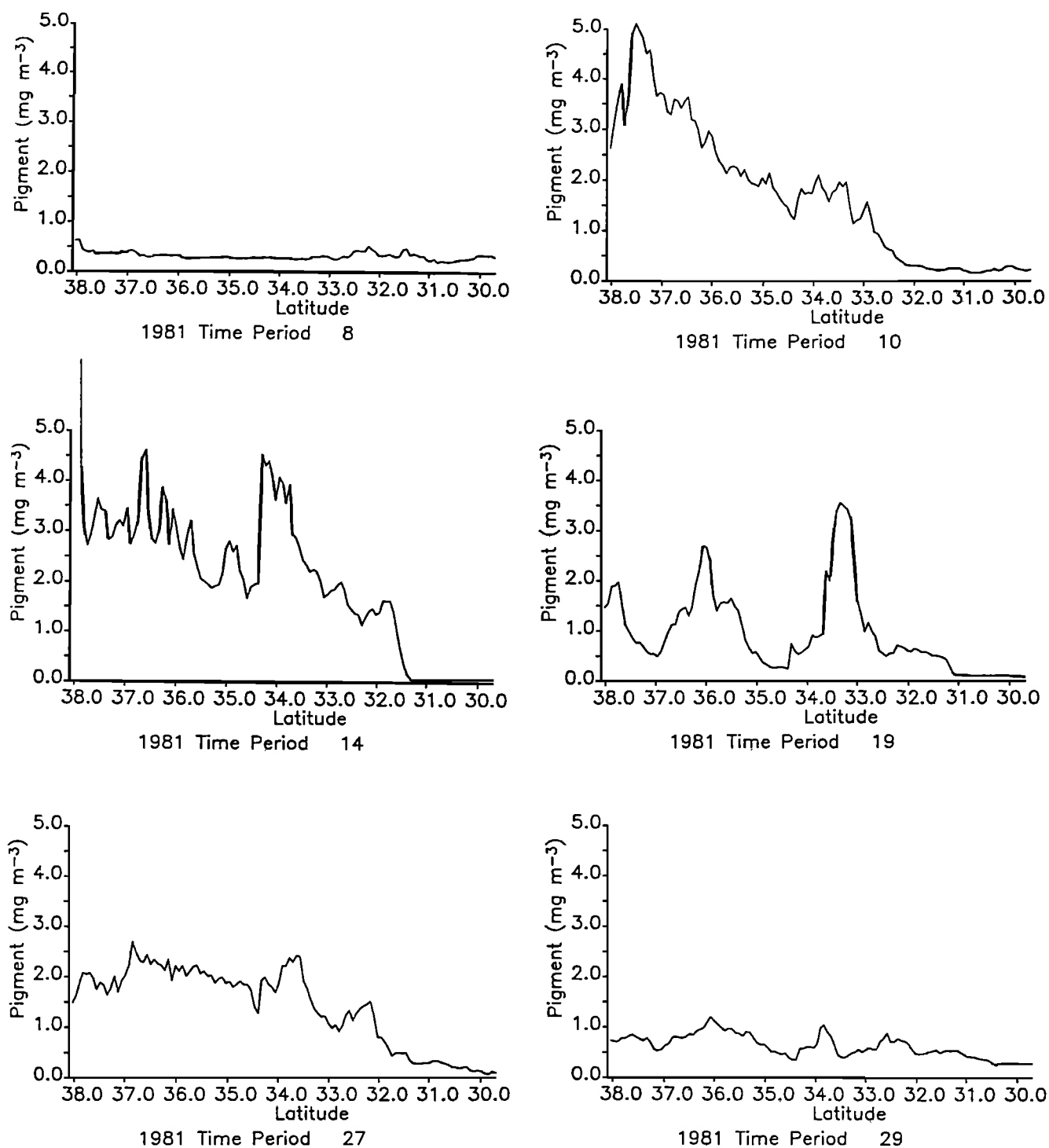


Fig. 3. Individual transects from periods in 1981 illustrating specific features of the seasonal cycle which reoccur in different years (see text): (a) period 8 (Julian days 71–80, March 12–21), (b) period 10 (Julian days 91–100, April 1–10), (c) period 14 (Julian days 131–140, May 11–20), (d) period 19 (Julian days 181–190, June 30–July 9), (e) period 27 (Julian days 261–270, September 18–27), and (f) period 29 (Julian days 281–290, October 8–17).

4. Concentrations north of the frontal zone decrease to between 0.5 and 1.5 mg m^{-3} in mid to late summer. Although this reduction is often less or delayed at latitudes centered at $\approx 33^\circ\text{N}$, the signature of the frontal zone weakens and periodically disappears.

5. The frontal zone is reestablished between $\approx 32^\circ\text{N}$ and

33°N for a brief period in the late summer (late August–September) by short time scale (20–40 days) increases in pigment concentration north of these latitudes.

6. This increase is followed by a sudden decrease (within 10 days) in concentrations at all latitudes north of $\approx 33^\circ\text{N}$. For this period in the fall (September or October), low

concentrations (often $<0.5 \text{ mg m}^{-3}$) are again present over the entire latitudinal range of the study area, and the frontal zone disappears.

Time period 8 (Julian days 71–80, March 12–21) in 1981 (Figure 3a) is an example of the low concentrations present over the entire transect in the early spring. They are never greater than 0.5 mg m^{-3} and there is no evidence of a frontal zone. Dramatic increases in pigment concentration take place in most years in the northern portions of the study area following this early spring period. The data from period 10 (Figure 3b) (Julian days 91–100, April 1–10) show concentrations greater than 3.0 mg m^{-3} at latitudes north of 36°N and concentrations greater than 1.5 mg m^{-3} extending south to $\approx 33^\circ\text{N}$. A strongly developed frontal zone is evident between 32°N and 33°N , separating these higher concentrations from concentrations less than 0.5 mg m^{-3} south of 32°N . Similar high concentrations are present in the north at period 14 (Julian days 131–140, May 11–20) (Figure 3c). The frontal zone is farther south ($\approx 31.5^\circ\text{N}$) and has a stronger gradient than at period 10. In addition (and not evident in the contour plot), pigment concentrations south of the front are lower than at previous times. Period 19 (Julian days 181–190, June 30 to July 9) (Figure 3d) illustrates the midsummer decline in pigment concentration seen in most years in northern portions of the transect. While concentrations south of the front remain low, concentrations north of $\approx 31^\circ\text{N}$ are less than 1.5 mg m^{-3} over most of the transect. The frontal zone, while still present, is considerably weaker and is farther south (just north of 31°N). Increases in concentration in the late summer in the northern portion of the transect reestablish the strong frontal zone at $\approx 32^\circ\text{N}$. This feature is illustrated in Figure 3e showing period 27 (Julian days 261–270, September 18–27). Data from this period also show that concentrations south of the frontal zone are slightly higher than the very low values seen in midsummer (Figures 3c and 3d). The fall decrease in concentrations over northern portions of the transect is illustrated in Figure 3f (period 29, Julian days 281–290, October 8–17). During this period the frontal zone is not evident in the satellite pigment data.

Although the purpose of this study is to examine latitudinal and temporal variability within the study region, the transects presented in Figures 2 and 3 obviously miss any longitudinal variability which would bias both the position and gradient of the front presented in Figures 2 and 3. *Peláez and McGowan* [1986] show that the two-dimensional attitude of the frontal zone can be quite variable. Ten-day composite images from 1981 are presented in Plate 1 to illustrate the two-dimensional structure of features in the study area common to most years. (Plate 1 is shown here in black and white. The color version can be found in the separate color section in this issue.) These images are from the same periods shown in Figure 3 to allow a comparison with both the individual transects and the temporal contours. Superimposed on the images in Plate 1 is the meridional spatial region within which the data were longitudinally averaged to produce the transects shown in Figures 2 and 3.

Plate 1a (period 8) shows that the low concentrations present in early spring in the study area are present over most of the CCS. In general, only regions within $\approx 20 \text{ km}$ of the coast have concentrations greater than

1.0 mg m^{-3} . The image composite in Plates 1b and 1c (periods 10 and 14) shows the spatial extent of pigment concentration increases characteristic of the late spring and early summer. This latter image does, however, show lower concentrations of pigment in the southern portion of the study area. The orientation of the frontal zone during both time periods is strongly east-west. Plate 1d (period 19) indicates that lower pigment concentrations in the northern portion of the transect in midsummer are due to spatial changes in the offshore distribution of pigment. The region influenced by higher concentrations has contracted eastward to within $\approx 100 \text{ km}$ of the coast except in specific areas where filaments of higher pigment concentration extend offshore. In the fall (period 27, Plate 1e), a diffuse region of increased concentration has expanded offshore in the northern portion of the study area with filaments evident only seaward of the study area and no intrusions of offshore, oligotrophic water apparent within the transect. The image for period 29 (Plate 1f) shows generally lower concentrations along the entire transect during this fall period and the reappearance of filaments with higher pigment concentration extending offshore through the sampled transect producing the strong latitudinal variability seen in Figure 3f. Higher concentrations in the southern portion of the study area, compared with those in midsummer, are evident. A tongue of higher pigment concentration extending down the western edge of the transect between $\approx 32^\circ\text{N}$ and 30°N alters the orientation of the frontal zone away from east-west and reduces the gradient of pigment concentration in the transects shown in Figures 2 and 3 for this time period.

3.2. Interannual Variability

Interannual variability of pigment concentrations in the transect is summarized by decomposing the time and space series into empirical orthogonal functions (EOFs). Suspect winter data in each year (marked in Figure 2) were not included in the calculation. Each mode of an EOF decomposition has a spatial pattern whose amplitude in time is represented by a time series. Original pigment concentrations associated with any one mode can be reconstructed by multiplication of the spatial value and the amplitude value at the time of interest. The original total pigment concentrations can be reconstructed by summation over all modes of this product. The first EOF mode, which accounts for 62.4% of the total variance, is presented in Figure 4. The second EOF mode accounts for less than 10% of the variance. This and higher modes are probably not statistically significant and are not presented here. The spatial pattern of the first mode shows relatively high values north of $\approx 32^\circ\text{N}$, a strong latitudinal gradient between $\approx 32.3^\circ\text{N}$ and 31.5°N , and low values south of 31.5°N . The temporal variability of this dominant pattern is shown by the amplitude time series (Figure 4). The seasonal cycle described previously is readily apparent, as is the interannual variability of these features.

Temporal development of this pigment pattern for the period in 1979 when data are available and throughout 1980 and 1981 closely follow the general seasonality described above. Most characteristics of the general seasonal cycle are present in 1982, but the magnitude and timing of specific features are different. The early spring period of low pigment concentrations occurs ≈ 20 days later in

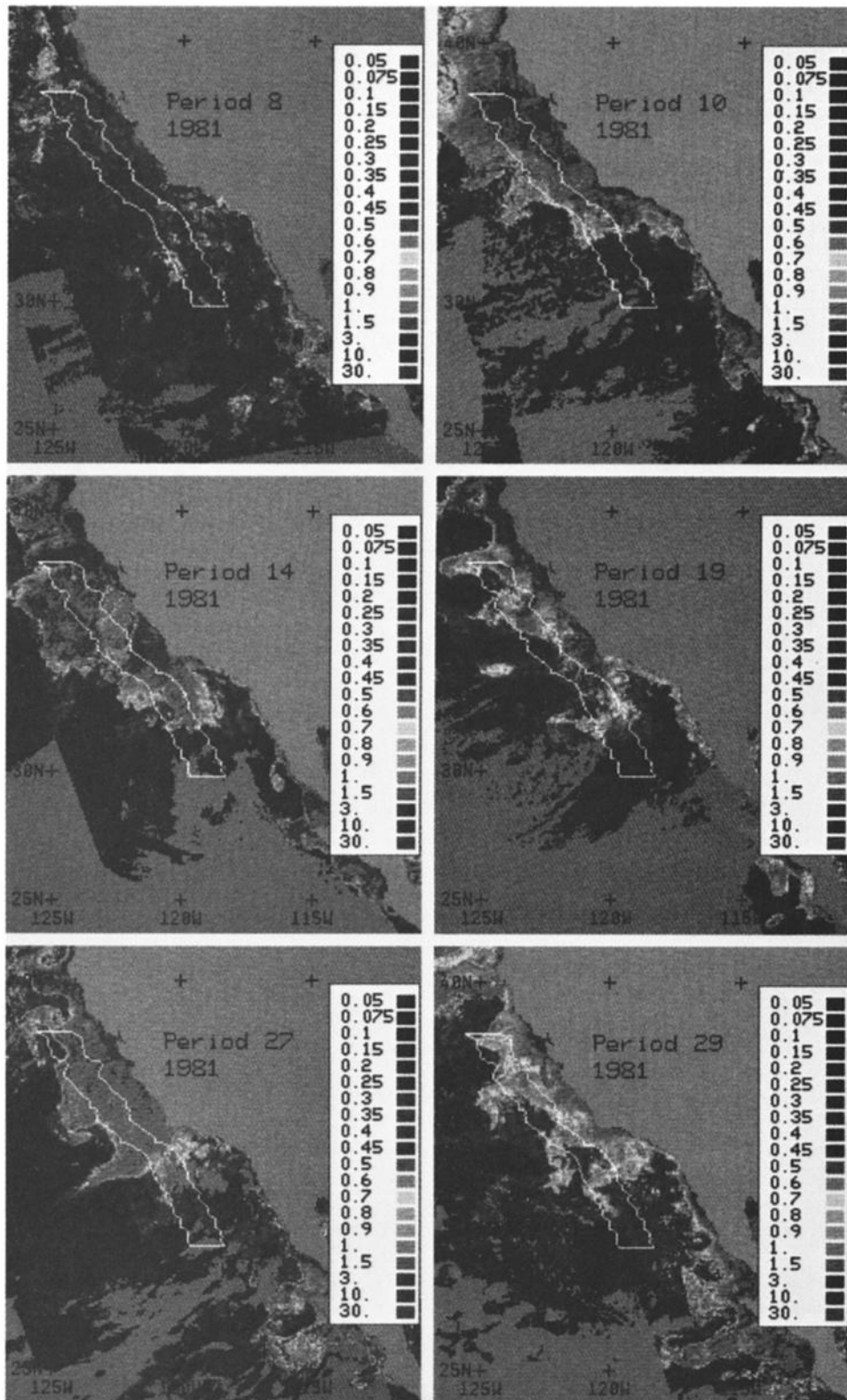


Plate 1. Ten-day composite CZCS images of the periods in 1981 shown in Figure 3. (The color version and a complete description of this figure can be found in the separate color section in this issue.)

the year than in 1980 and 1981 (compare also these time series in Figure 2). The spring increase in concentration at latitudes north of $\approx 32^\circ\text{N}$ following this period is considerably smaller in both latitudinal and temporal

extent than in previous years and appears as a series of episodic increases. Examination of Figure 2d shows that these increases take place north of $\approx 36^\circ\text{N}$ from the beginning of April until June. In the summer and fall,

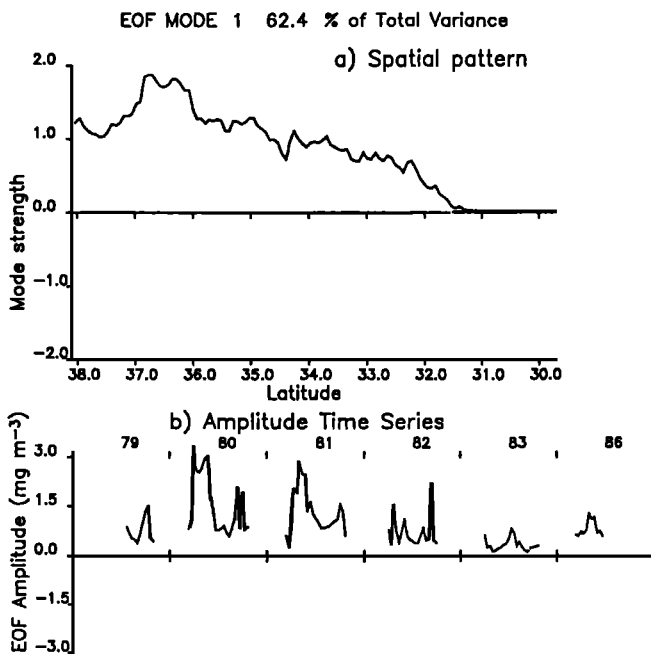


Fig. 4. The first EOF mode (a) spatial pattern and (b) amplitude time series of the meridional transect in Figure 1 over the 6 years of WCTS data presented in Figure 2. Note that winter data from the periods assumed to be affected by the atmospheric correction error (marked in Figure 2) are not included in the decomposition.

the 1982 time series in Figure 4 is similar to the general seasonal pattern but the fall increase begins in mid-August, 20–30 days earlier than previous years. Figure 2d shows that oligotrophic conditions extend farther north than in previously examined years, with the frontal zone remaining at $\approx 33^\circ\text{N}$ throughout the summer. In 1982 the frontal zone is weak throughout the summer except for a period in early June and again in the period leading up to the fall increase. Summer concentrations in the northern portion of the transect are lower than those of previous years (generally $< 0.5 \text{ mg m}^{-3}$).

The time series in 1983 (Figure 4) is very different from the general seasonal pattern. While concentrations along the entire transect are low in the earliest part of the year, no subsequent spring or fall increase in concentration takes place. The largest amplitudes of the spatial pattern occur in midsummer but are still lower than those of other years. Figure 2e shows that oligotrophic conditions dominate the study area throughout the spring, summer, and fall. The increase in concentration between 32°N and 35°N in early June briefly establishes a frontal zone which lasts until mid-July, although for most of this time the gradient is weak. A short time scale increase takes place north of 36°N in July with concentrations of $> 2.0 \text{ mg m}^{-3}$. With these episodic exceptions, pigment concentrations remain less than 0.5 mg m^{-3} from mid-March until mid-October (the entire period for which 1983 data are considered valid) over the whole study area.

The time series from 1986 (Figure 4) indicates that the spring increase is relatively weak and occurs relatively late in the spring. Figure 2f indicates that the spring increase in pigment concentration occurs primarily north of $\approx 36^\circ\text{N}$ and that the frontal zone between 32° and 33°N is weaker than that evident in 1980 and 1981.

4. DISCUSSION

4.1. Comparison With Previous Work

The reduction in pigment gradient across the front in late summer pointed out by Peláez and McGowan [1986] using individual images is evident in our analysis of the entire data set of CZCS images. The temporal progression of the frontal zone described in the preceding section (see Figure 2), however, differs from that described by these authors. They describe a continual southward movement of the front, starting in spring, and reaching its southern most position in August or September. In Figure 2 the frontal zone moves southward in the spring (in 1980 and 1981) but reaches its most southerly position in May–June. Thereafter, the frontal gradient is weaker and moves northward until the brief fall pigment increase. Peláez and McGowan also describe interannual variability in different seasons from an analysis of an individual image from each of 3 years. They describe similar summer (July) patterns in each year (1979, 1980, 1981). This similarity is also evident in our data (Figure 2) and appears to be true of 1982 as well. However, they describe spring (April) conditions in 1980, 1981, and 1982 as being remarkably similar. This is not true of patterns evident in Figures 2 and 5. Both the actual concentrations and the spatial-temporal extent of higher pigment concentrations in the spring of 1982 are less than those of 1980 and 1981. This agrees with the interannual variability of pigment patterns during the spring discussed by Thomas and Strub [1989]. Differences between the seasonality and interannual variability described here and those discussed by Peláez and McGowan may be due to a number of factors. These authors use only 21 images, selected on the basis of being extensively cloud free, and base their discussion on these individual images. They interpret color patterns rather than the actual pigment concentrations contoured here. Their visual interpretation also might differ in location, including patterns extending into the bight, whereas our transect is restricted to the same geographic region throughout the year. Although our spatial temporal averaging eliminates smaller scale features, we argue that use of the entire data set resolves the large-scale patterns and seasonal variability better than a small group of hand-selected images, which may alias episodic or short-term changes into an apparent seasonal evolution.

4.2. Comparisons With in Situ Data

Unfortunately, few in situ biological data from the CalCOFI program coincide with the CZCS data presented here, and other sampling programs do not have the spatial and/or temporal coverage necessary for a meaningful comparison. A cruise from 1981 and a comprehensive series of cruises in 1984, however, provide an illustration of surface and subsurface hydrographic and biological characteristics in the study area. The extent to which these data reflect patterns in the years covered by the WCTS is unknown, although subsurface hydrographic data collected on cruises in February and April 1980 [SIO, 1985a] (not shown) indicate patterns similar to those described below.

The extent to which the patterns shown in Figures 2–4 are influenced by changes in the vertical distribution of chlorophyll is difficult to assess, owing both to the lack of concurrent in situ data and to the fact that spatial and temporal patterns are hard to separate and often

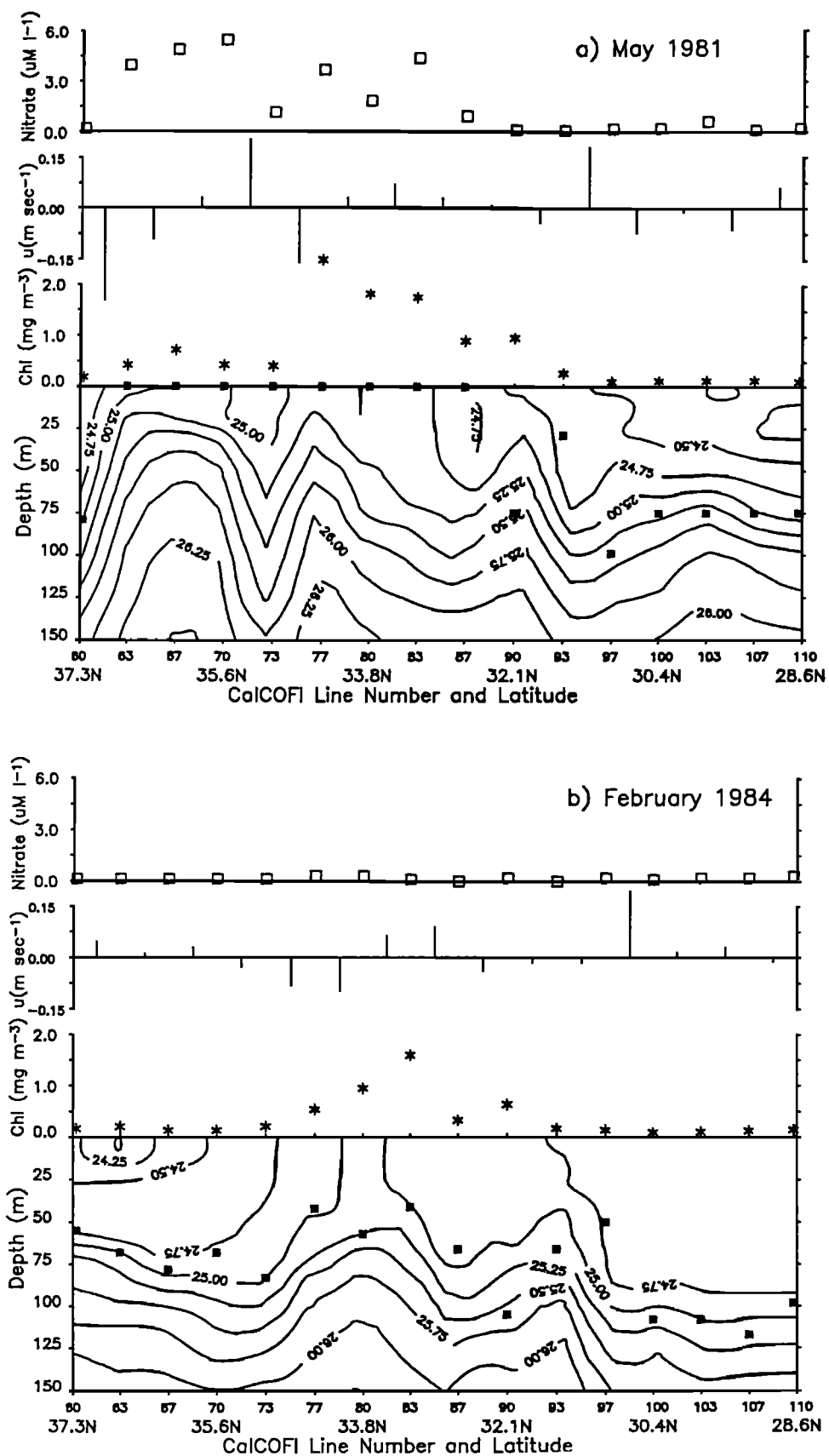


Fig. 5. Vertical contours of density structure through station 70 (see Figure 1) on each CalCOFI line from CalCOFI cruises (a) 8105, (b) 8402, (c) 8404, (d) 8405-06, (e) 8407, and (f) 8407. The first two digits indicate the year, and the last two, the month of the cruise. Shown as solid squares on the contour plot is the depth of the nitracline (defined as the shallowest depth at which nitrate concentrations are $> 0.5 \mu M$). Also shown are pigment concentrations (chlorophyll plus phaeopigments) at the surface (usually 1-3 m), cross-shelf geostrophic velocities (0/500m) and surface nitrate concentrations (arrows indicate concentrations $> 7.0 \mu M$).

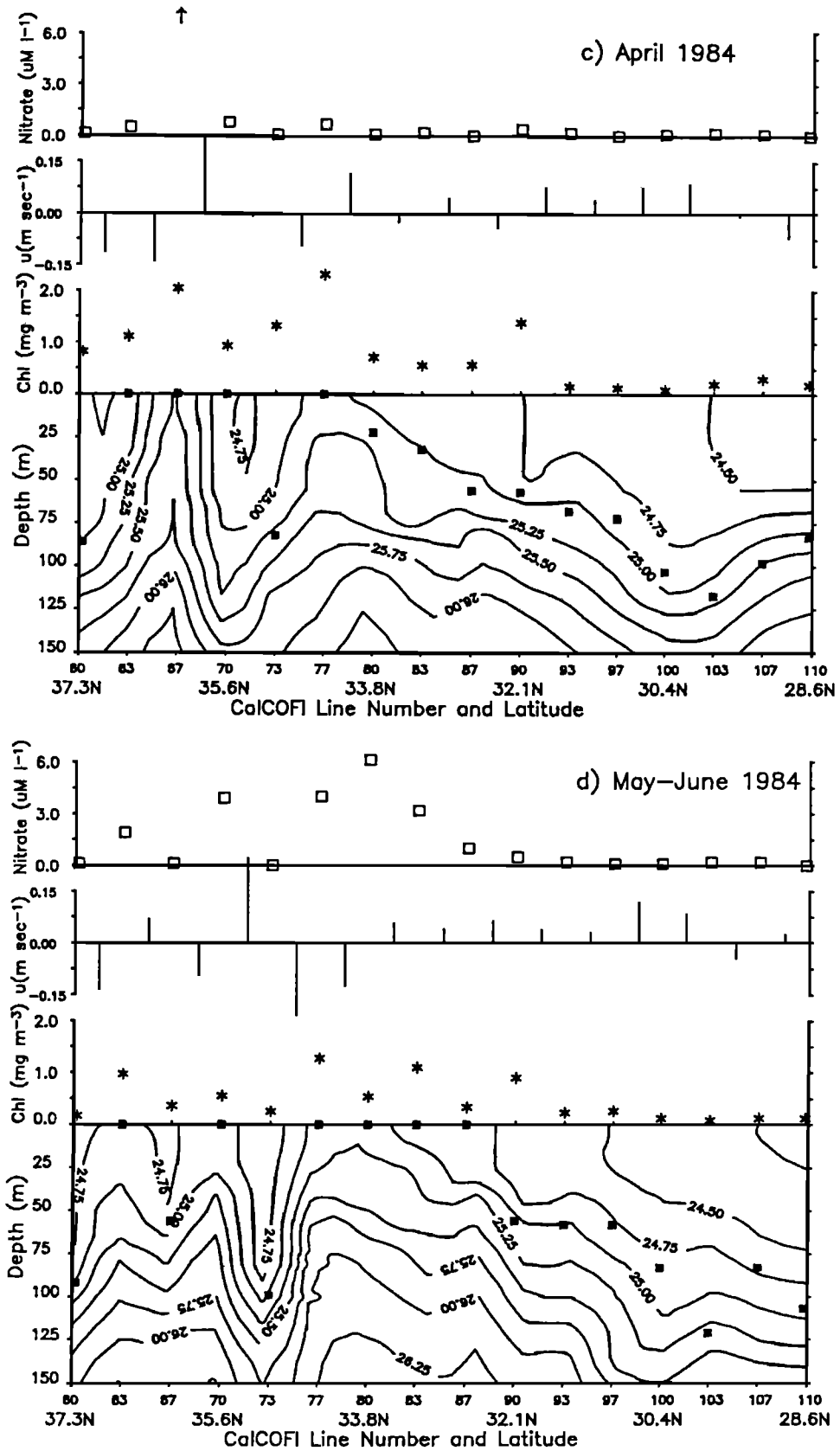


Fig. 5. (continued)

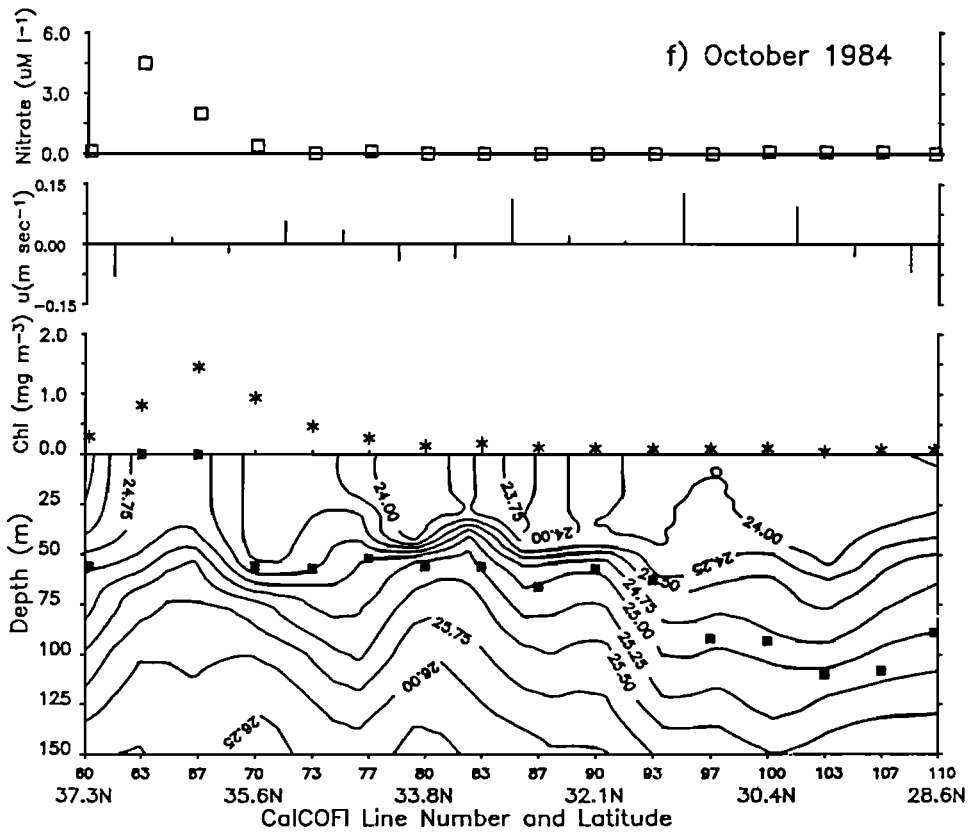
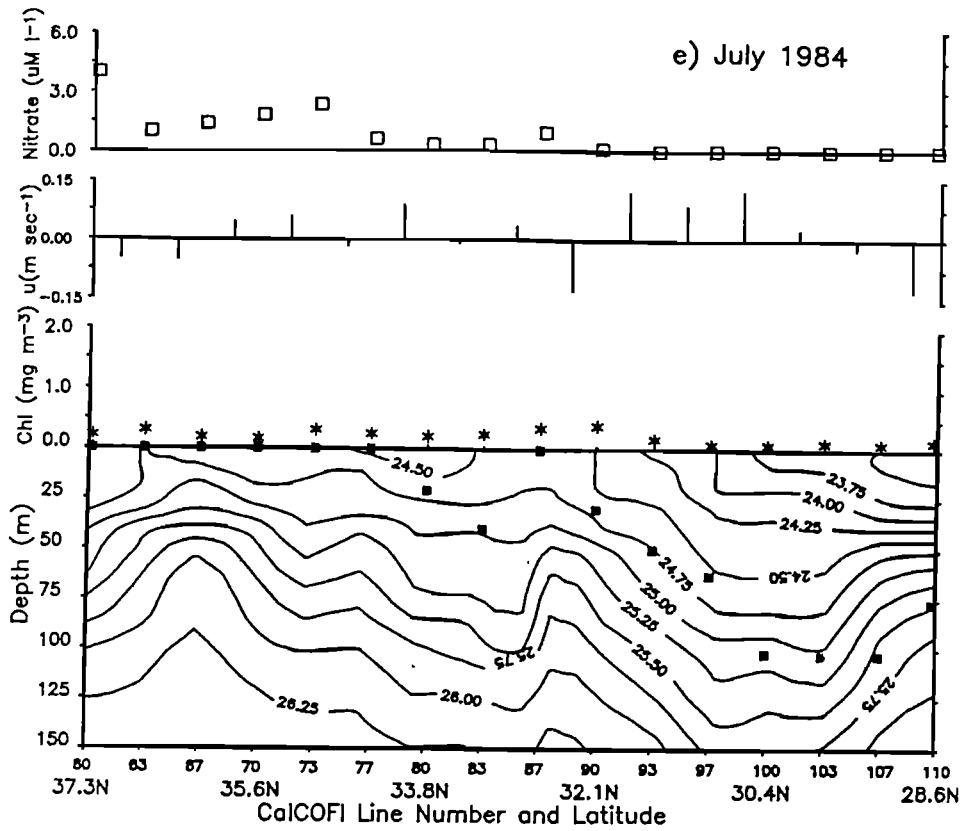


Fig. 5. (continued)

not resolved in the CalCOFI data. For regions south of the frontal zone, in which surface concentrations are always low (Figure 2), and the nitracline (defined here as the shallowest depth at which nitrate concentrations were $\geq 0.50 \mu\text{M}$) and pycnocline are relatively deep all year (Figure 5), the presence of a subsurface chlorophyll maximum at depths deeper than ≈ 60 m (1984 CalCOFI data; not shown) probably has little influence on the pigment concentrations measured by the satellite. This argument is less valid in regions north of the front where high pigment concentrations are present in the spring and the pycnocline, nitracline, and subsurface chlorophyll maximum (not shown) are often relatively shallow (Figure 5). Temporal changes in the vertical distribution of chlorophyll, such as sinking in the late spring or vertical mixing in the fall, could induce spatial pattern in the upper attenuation depth integrated by the CZCS. *Hayward and Venrick* [1982] show that total water column chlorophyll concentrations are strongly correlated with surface concentrations in the CCS. The 1984 CalCOFI data indicate that in general, the subsurface chlorophyll maximum north of the front is deeper than 20 m over the whole year and probably is not seen by the CZCS. The position of the frontal zone evident in the CZCS data is closely related to that in hydrographic and other biological data, as is discussed in the introduction. These factors argue that surface pigment patterns seen by the CZCS are not strongly biased by temporal changes in vertical distribution. The fact remains, however, that the CZCS measures only those pigments in the upper water column, and these need not reflect total water column concentrations. Spatial and temporal patterns evident in Figures 2–4 should not be interpreted as those of total water column biomass.

4.2.1. *Spatial structure.* Contours of subsurface density along a transect similar to that used to sample the CZCS image composites (station 70 from CalCOFI lines 60 to 110) from the 1981 cruise and the five cruises in 1984 are plotted in Figure 5 along with the depth of the nitracline and surface "pigment concentration" (chlorophyll plus phaeopigment concentration). The location of these stations is shown in Figure 1.

The contours of subsurface density in Figure 5 indicate the presence of a hydrographic frontal zone at latitudes similar to those where pigment gradients are strongest in the satellite data, a relationship supported by the previous observations of *Peláez and McGowan* [1986] and *Niiler et al.* [1989] and long-term averages of density structure [*Lynn et al.*, 1982]. In each of the months presented, dense water is relatively deep in the southern portion of the transect, shelves at a frontal zone located between lines 100 and 93 ($\approx 31.5^\circ\text{N}$) and is relatively shallow north of $\approx 32^\circ\text{N}$. In both February and October (Figures 5b and 5f), the frontal zone is primarily a subsurface feature, and a well-mixed surface layer eliminates any latitudinal gradient at depths shallower than ≈ 50 m. The data from these cruises suggest that a hydrographic expression of the frontal zone is present throughout the year, at least in 1984. Analysis of dynamic height over longer time scales [*Lynn et al.*, 1982; *Roesler and Chelton*, 1987] indicate that this is a recurring feature of the CCS in this region. Data from May 1981 show a pattern similar to that of May–June 1984, as do data from

February and April 1980 (not shown). We thus take the features evident in the 1984 data to be representative of normal conditions.

Profiles of cross-shelf geostrophic velocity (relative to 500 m) included in Figure 5 indicate the surface flow associated with the subsurface density field. Strong ($> 10 \text{ cm s}^{-1}$) onshore flow usually occurs between 29°N and 32°N , over the main frontal zone, in agreement with the previously mentioned studies. Especially in April and May–June (Figures 5c and 5d), strong horizontal density gradients in the northern portion of the transect are evidence of intense cross-shelf flows characteristic of the CCS during the summer [*Mooers and Robinson*, 1984; *Kosro*, 1987] and similar to the filaments visible in Figure 4. Although the CalCOFI grid spacing does not adequately resolve these features, the data indicate that north of 32°N , higher pigment and nutrient concentrations and a shallower nitracline are often bracketed by offshore flow to the north and onshore flow to the south (especially in February, April, and May–June). This is consistent with the conceptual model of a meandering southward jet within the CCS, with eutrophic water inshore and more oligotrophic water offshore of the jet.

The biological implications of this subsurface density structure are seen in the depth of the nitracline and surface in situ pigment and nitrate concentrations at each station along the transect (Figure 5). In a nutrient-limited system, the relationship between the depth of the nitracline and the depth of the euphotic zone is evidence of the extent of physical forcing and nutrient availability for phytoplankton growth in the upper part of the water column. Oligotrophic regions are generally characterized by reduced physical forcing with upper water column primary production in approximate equilibrium with nutrient regeneration. The flux of new nutrients into the upper water column is relatively low. In these regions the nitracline and euphotic zone depth will be similar and are usually relatively deep. Regions where the nitracline is relatively shallow compared with the depth of the euphotic zone have been disturbed from this equilibrium. These are regions where recent physical forcing has introduced new nutrients into the euphotic zone and are generally more eutrophic, conditions characteristic of eastern boundary currents. Wind forcing resulting in coastal upwelling [*Huyer*, 1983; *Traganza et al.*, 1987; *Jones et al.*, 1983], Ekman pumping [*Chelton*, 1982; *Strub et al.*, 1990], and vertical mixing [*Husby and Nelson*, 1982; *Thomas and Strub*, 1989] have all been shown to influence the productivity in the CCS. During summer, coastal upwelling is characteristic of the entire region.

In each of the months presented, the depth of the nitracline becomes shallower at the frontal zone coincident with the shoaling isopycnals. During the spring and summer cruises, the nitracline and surface pigment and nitrate concentrations are higher in the northern portions of the transect. The February and October cruises (winter and fall) do not show increased pigment concentrations at the frontal zone. In May 1981 and in May–June and July 1984, the nitracline actually outcrops the surface at line 87 and stations farther north. South of the frontal zone, the nitracline is typically at or below 100 m. Surface pigment concentrations are always less than 0.5 mg m^{-3} and often less than 0.25 mg m^{-3} south of the

frontal zone, indicative of an oligotrophic water column and consistent with the patterns of satellite-measured pigment concentration presented in Figure 2.

Changes in pigment concentration along the transect shown in Figure 2 are a close approximation of changes within what *Lynn and Simpson* [1987] describe as a transition zone in the CCS. This transition zone is in the high-speed core of the CCS which the authors characterize as being dominated by mesoscale eddies and meanders. The images shown in Plate 1 indicate that most of the latitudinal variability illustrated in Figures 2 and 3 is due to such mesoscale features oriented in a cross-shelf direction and associated with strong cross-shelf flow [*Moore and Robinson*, 1984; *Kosro*, 1987] described above. The WCTS CZCS data presented in Figure 2 suggest that the most temporally stable feature in this transition zone is a tongue of higher pigment concentration located more than 200 km offshore of the SCB between $\approx 32.5^\circ\text{N}$ and 34°N . This is immediately "downstream" of Point Conception, a region of strong and persistent upwelling [*Brink et al.*, 1984; *Atkinson et al.*, 1986] suggesting that advection of nutrients and biomass from this upwelling region might play a role in the patterns evident in Figure 2, as was implied by *Haury et al.* [1986].

4.2.2. Temporal structure. The seasonal pattern evident in Figures 2 and 4 cannot be compared directly to the in situ data on account of the mismatch in years, spatial resolution and synopticity of sampling; obviously, these in situ data will not allow an examination of interannual variability. The in situ data from 1984 do, however, illustrate two features of the seasonal pattern seen in the satellite data. In addition, previously published hydrographic and biological data from 1983 allow explanations of the highly anomalous pigment concentrations and patterns in this year.

The mid-late summer decrease in surface pigment concentrations north of $\approx 33^\circ\text{N}$ evident in the satellite data in 1979–1982 (Figure 2) is supported by the July in situ measurements from 1984 (Figure 5e) in which concentrations are lower north of the front ($< 0.5 \text{ mg m}^{-3}$) than those of either May–June or April. Spatial patterns in the satellite imagery of 1981 suggest that reduced pigment concentrations within the transect in mid-late summer are due to a retreat of higher biomass toward the coast (contrast Plates 1c and 1d). Comparisons of the mean cross-shelf distribution of pigment in a zonal transect (see Figure 1) in spring and summer (Figure 6) show that this onshore redistribution is a recurring feature of the CCS at this latitude ($\approx 35^\circ\text{N}$ to 38°N). Regions of higher pigment concentration extend ≈ 500 km offshore in the spring (April–May) of 1980 and 1981 and ≈ 300 km offshore in the spring of 1982 and 1986. In contrast, higher concentrations in summer (June–July) are restricted to within 100–200 km of the coast. The exception to this trend is 1983, when regions of higher pigment concentration do not extend farther than 200 km offshore during either spring or summer. Subsurface density structure suggests that this contraction of pigment concentration toward the coast as the summer progresses is accompanied by an increase in vertical stratification in the region of the sampled transect (contrast the stratification in the upper 50 m in Figure 5c and 5d with 5e) which would reduce the vertical flux of nutrients into the upper water column. A comparison of the buoyancy frequency N

of the upper 50 m over three of the 1984 cruises, averaged within each cruise over each station where the nitracline outcrops the surface (see Figure 5), is 0.045, 0.064, and 0.086 rad s^{-1} for April, May–June, and July, respectively. The density difference over the top 50 m is almost twice as strong in July as it is in May–June. Reduced vertical flux is also implied by the surface nutrient concentrations at these stations. Although the nitracline outcrops the surface (by our definition) at seven northern stations in July (Figure 5e), mean surface nitrate concentrations are only $1.7 \mu\text{M}$ compared to $3.5 \mu\text{M}$ during May–June. If other factors are assumed constant, the July nutrient concentrations would support approximately half the phytoplankton biomass that concentrations in May–June would. Reduced biomass in midsummer is also supported by phytoplankton growth rates. A comparison of the depth averaged vertically integrated primary productivity in the euphotic zone (approximately the 1% light level) at stations north of the frontal zone over the same CalCOFI cruises shows that rates are considerably lower in July (a mean of $1.2 \text{ mgC m}^{-3} \text{ h}^{-1}$) than in either April or May–June (means of 5.2 and $3.7 \text{ mgC m}^{-3} \text{ h}^{-1}$ respectively). The high productivity in April might explain the presence of high chlorophyll concentrations in association with relatively low nitrate concentrations present in the spring. While this discussion is internally consistent, the data do not explain why the productivity in May–June is less than that in April despite relatively high nutrient concentrations at the surface.

The mechanisms responsible for this summer onshore redistribution of pigment concentration are not clear. Preliminary results from the Coastal Transition Zone (CTZ) experiment indicate that high phytoplankton biomass, originating nearshore in upwelling regions, is usually associated with the inside or nearshore region of the meandering velocity structure making up the mesoscale filaments observed in satellite imagery [*A. Huyer and T. Cowles, personal communication*, 1989]. This suggests that the offshore extent of high pigment derived from coastal upwelling would be controlled by the cross-shelf location of the high velocity core of the CCS. This is supported by data in Figure 5 and by the similarities of dynamic height and chlorophyll concentration shown in the CalCOFI data reports. The seasonality of the cross-shelf position of velocity structure in the CCS [*Lynn and Simpson*, 1987], however, shows an opposite trend to that seen in the CZCS data over most of the latitudinal range of our mean cross-shelf transect (see Figure 1). Their data (a long-term average of geostrophic velocities perpendicular to CalCOFI lines) show the main core of the CCS farther offshore in June–July than in April–May. Only in the most northern portion of the study area does the core of the CCS shift onshore during the May–July period. It is possible that in such a dynamic system the long-term average presented by these authors smoothes the actual cross-shelf current structure beyond the point where a meaningful comparison can be made. Although these data are not concurrent, they do suggest that control of the cross-shelf extent of high pigment concentrations might not be due to current structure at all times of the year.

The data presented above are consistent in suggesting that current structure might be important in mid-late

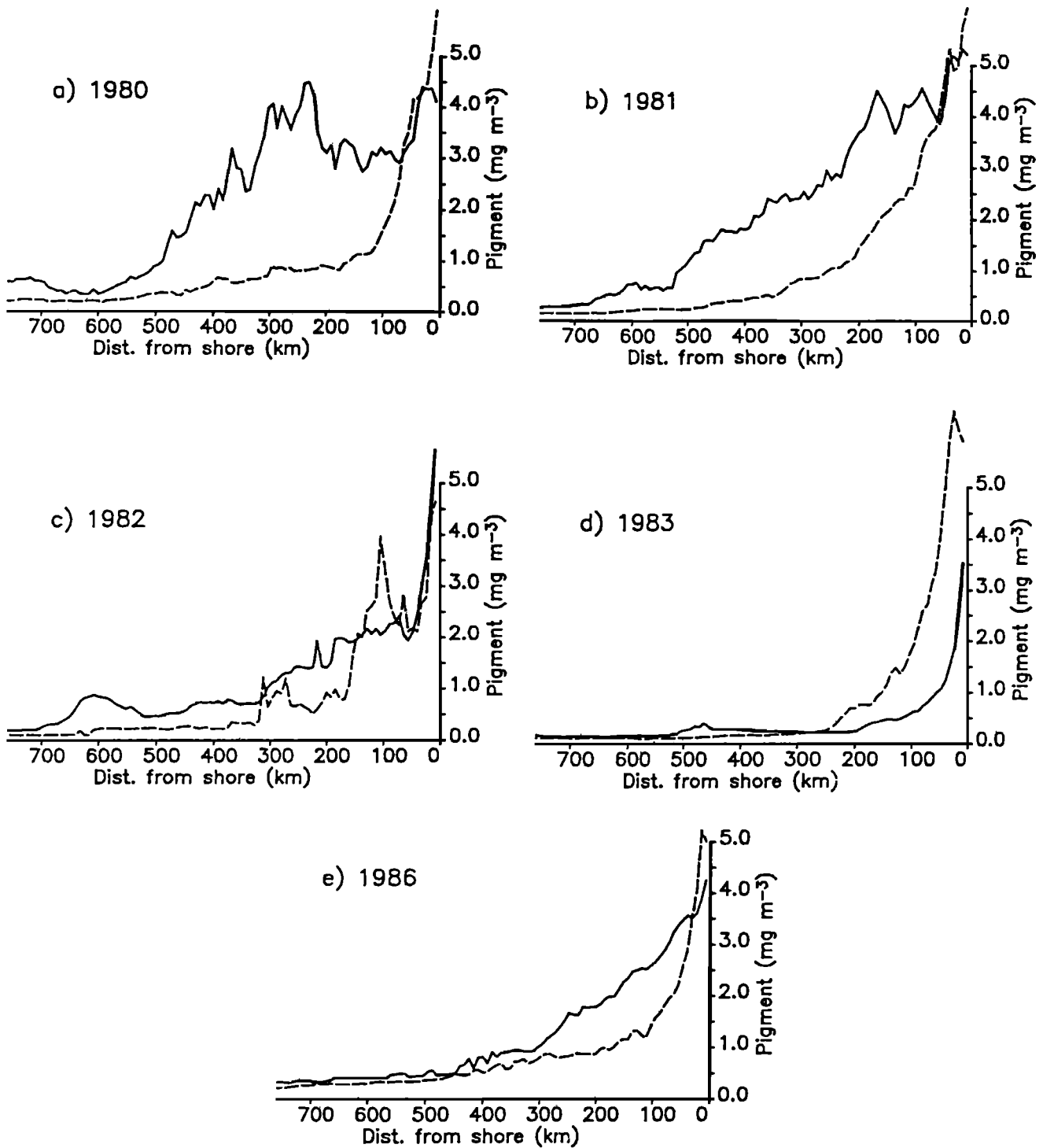


Fig. 6. The mean cross-shelf distribution of pigment concentration over the latitudinal range shown in Figure 1. Shown for each year is a mean for three 10-day periods in the spring (beginning April 11) as a solid line and a mean for three 10-day periods in the summer (beginning June 10, except 1986 May 21), as a dashed line.

summer when stratification in the central and offshore CCS is the strongest and coastal upwelling is the primary source of nutrients and resultant higher phytoplankton biomass. *Thomas and Strub* [1989] show that in the winter and spring, vertical mixing by wind events can lead to increases in pigment concentration over large portions of the CCS, extending up to 700 km offshore in a diffuse

spatial pattern very different than the filaments and eddies seen in the later summer. It is possible, then, that in the early portion of the year, vertical nutrient fluxes by other mechanisms, in addition to upwelling, are important. At this time, resultant biological distributions do not have a strong resemblance to the current structure. As the summer progresses, the offshore water column becomes

increasingly stratified, nutrients are depleted, regeneration cannot support the biomass, and cells sink out of the upper water column. Nutrient flux in the upper water column and spatial patterns of phytoplankton biomass become increasingly dominated by coastal upwelling and the current structure of the CCS. This hypothesis cannot be tested with the data presently available and awaits a more detailed sampling of both biological and physical variables over seasonal time scales.

The in situ data from October 1984 (Figure 5f) appear to illustrate conditions during a fall period of relatively low pigment concentration in northern portions of the transect similar to those evident at the end of each year in Figure 2. Surface in situ pigment concentrations are $< 0.5 \text{ mg m}^{-3}$ at all stations south of $\approx 35^\circ\text{N}$, and no surface chlorophyll gradient is present in the vicinity of $\approx 32^\circ\text{N}$. Mean concentrations are slightly less than those evident in Figure 3f (period 29, 1981); however, maxima in both data sets are similar ($\approx 1.5 \text{ mg m}^{-3}$). Plate 1 shows that spatial patterns of pigment at this time (period 29) are similar to those of mid-late summer (period 19) but that concentrations are 2–3 times lower. In this early fall period, the upper 50 m of the water column is well mixed (Figure 5f) and the pycnocline both relatively strong and deep compared to previous cruises (except at two northern stations where cross-shelf flow is evident). The nitracline is also relatively deep and often below the pycnocline, isolating surface water from nutrient enrichment. Mean depth-averaged vertically integrated primary productivity for stations north of the (subsurface) front in October 1984 is $1.0 \text{ mgC m}^{-3} \text{ h}^{-1}$, similar to that of July but less than those of April and May–June (see above). During this period the frontal zone is a subsurface feature, and oligotrophic conditions characteristic of the southern portion of the study area are present in the upper water column as far north as 35°N .

Changes in pigment concentration within the northern portion of the meridional transect during this latter portion of the year (period 29 in Figure 3 and Plate 1) appear to result from both a change in cross-shelf distribution of biomass and a change in actual concentration (contrast periods 27 and 29 in Plate 1). Changes in the cross-shelf distribution of biomass both during the fall increase and during the late-fall decrease are difficult to compare to climatologies of geostrophic current structure due to the short time scale of these pigment features (10–20 days, see Figure 2). Published presentations of the cross-shelf current structure [Lynn and Simpson, 1987; Roesler and Chelton, 1987] use monthly means which do not resolve such short-term changes. Furthermore, such spatial structure might be lost in these long-term averages. The late-fall periods of low pigment concentration appear to occur at the same time as a change in nearshore current direction. Chelton [1984] shows that surface currents within $\approx 75 \text{ km}$ of the coast change from southward (throughout spring and summer) to northward in October (and throughout winter). Again, Chelton's data are long-term averages and not directly comparable. It does suggest, however, that in October, surface water near the coast has its source to the south rather than the north and might have different chemical and biological characteristics. Roemmich [1989] highlights the importance of horizontal nutrient advection in this region, especially close to the coast.

The El Niño of 1983 is associated with anomalous biological and hydrographic conditions all along the west coast of North America [McGowan, 1985; Norton *et al.*, 1985; Huyer and Smith, 1985]. Thomas and Strub [1989] show that the changes in spatial pattern and concentration of pigment in 1983 at the time of the spring transition are the smallest of the 5 years of CZCS data they examine. A comparison of a spring image of the SCB from 1982 with one from 1983 by Fiedler [1984] shows that pigment concentrations are both lower and more closely associated with the coast in 1983. The time series shown in Figures 2e and 4 show that anomalously low concentrations were characteristic of the study region over the whole year. Published in situ data suggest that these lower concentrations are due to stronger stratification and anomalously deep pycnocline and nutricline associated with the 1982–1983 El Niño [Rienecker and Mooers, 1986; Simpson, 1983; McGowan, 1985]. The low pigment concentrations are probably not due to reduced wind forcing. Rienecker and Mooers [1986] show that the monthly averaged Bakun upwelling index at 36°N in 1983 does not differ significantly from long-term means. Simpson [1984b] argues that these anomalies are a result of increased onshore transport of subarctic water from the offshore portions of the CCS. These conditions within the water column are consistent in suggesting that a reduced vertical nutrient flux into the euphotic zone in 1983 resulted in reduced primary productivity and biomass over large regions of the CCS.

4.3. Relationships to Wind Forcing

Three indices of wind forcing (wind stress curl, alongshore wind stress, and wind mixing (u_*^3)) at two locations representing the northern and southern portions of the meridional transect (see Figure 1) were calculated for each of the years of the WCTS. Examination of the time series in each year, however, indicated that most features of the interannual variability evident in the pigment data (Figures 2 and 4) could not be explained by these wind products. This is consistent with the statistical analysis of monthly anomalies in CZCS pigment concentrations by Strub *et al.* [1990], who found that only 25% of the pigment variance could be explained by wind forcing. Some features of the seasonal and spatial variability did appear to be more closely coupled to wind forcing, and in Figure 7 we present the 6-year mean [1979–1983, 1986] of these wind products.

The dominant feature of these data is the lower wind forcing and reduced seasonality over the southern portions of the transect compared with the northern portions. This supports the previously discussed relationship between nutricline depths (Figure 4) and the influence of physical forcing and reflects the relative seasonality of pigment concentrations in these portions of the study area.

Alongshore wind stress in the north of the transect (Figure 7) is generally less in July and August than in April and May. Strub *et al.* [1987a] show this to be characteristic of the entire California coast. Reduced upwelling in the mid-late summer might explain the reduced offshore extent of higher biomass shown in Figure 6.

The coincidence of the date of the spring transition in current and wind structure along the west coast (Table 1) and the timing of the spring increase in pigment

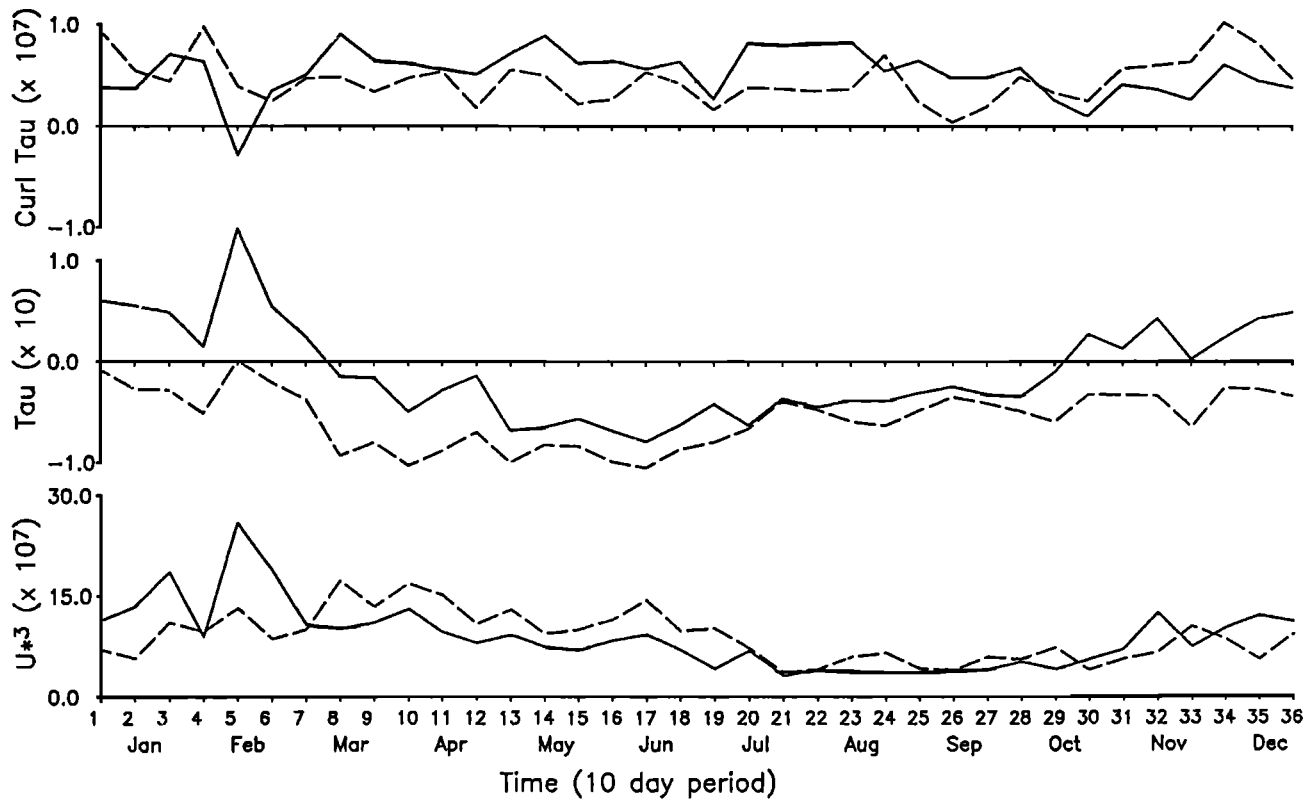


Fig. 7. Wind forcing from LFM data, characterized as u_*^3 , alongshore wind stress and wind stress curl averaged from daily values to 10 day means, and then averaged over 6 years (1979–1983, 1986), at a station representing the northern (solid line) and the southern (dashed line) portions of the meridional transect (see Figure 1).

TABLE 1. The Spring and Fall Transition Dates With Julian Days and the 10-Day Period in Which They Occur

Year	Spring			Fall		
	Date	Julian Day	Period	Date	Julian Day	Period
1980	March 22	82	9	Oct. 25	298	30
1981	March 26	85	9	Oct. 27	300	30
1982	April 18	108	11	Oct. 13	287	29
1983	April 4	94	10	Oct. 30	303	31
1986	March 17	77	8			

concentrations north of $\approx 33^\circ\text{N}$ (Figure 2) indicates a strong relationship between phytoplankton growth rates and wind forcing during this period in most years. The spring transition marks the seasonal change from northward mean wind stress and downwelling at the coast to southward mean wind stress and upwelling [Huyer *et al.*, 1979], seasonality evident only north of $\approx 34^\circ\text{N}$ [Strub *et al.*, 1987b]. A more detailed explanation of the dates chosen for the spring and fall transitions are given by Strub and James [1988] and Thomas and Strub [1989]. Thomas and Strub show that large spatial scale changes in pigment concentration can be associated with this physical event, but they emphasize the interannual variability of both spatial and temporal patterns in the CZCS imagery. This variability is evident in March–April data shown in Figure 2. These authors argue that because the water column in offshore regions

south of $\approx 40^\circ\text{N}$ is vertically stratified and nutrient depleted in late winter, interannual variability is due not only to differences in alongshore wind stress (upwelling) but also to the strength and timing of wind mixing events.

The wind data do not provide an explanation for the increase in pigment concentrations in the fall in the northern portion of the transect. This increase appears to occur at a time of reduced wind mixing and alongshore stress. Furthermore, no consistent relationship is evident between the date of the fall transition in wind and current structure (Table 1) (the switch from mean southward alongshore wind stress to northward) and the fall decrease in pigment concentrations or elimination of the frontal gradient seen in Figure 2. A detailed analysis of pigment temporal patterns and large-scale forcing in the fall is beyond the scope of this study and probably requires a

more complete time series of in situ biological and chemical measurements concurrent with hydrographic data than are available to us.

5. SUMMARY

Analysis of the complete CZCS data set from 6 years (1979–1983, 1986) illustrates the seasonal and interannual variability of near-surface phytoplankton pigment concentrations along an offshore meridional transect in the CCS from $\approx 38^\circ\text{N}$ to $\approx 30^\circ\text{N}$. Concentrations in winter were not analyzed on account of errors in the atmospheric correction algorithm used to process the satellite data. The transect crosses a semipermanent frontal zone which is also evident in in situ hydrographic data, illustrating the variability in the latitudinal position and relative gradient of pigment concentrations across the front. Seasonality is strongly developed in the region north of the front ($\approx 32^\circ\text{N}$) but virtually absent in water to the south. The seasonal development of higher concentrations in the northern portion of the transect determines the strength and latitudinal position of the frontal zone as expressed in pigment concentration.

A number of features in the time series of pigment concentrations recur in different years, and a generalized seasonal cycle is apparent, superimposed on interannual variability. This seasonal cycle shows low early spring concentrations throughout the latitudinal range of the transect and a late spring increase in concentration north of $\approx 32^\circ\text{N}$ which forms a zonally oriented frontal gradient. Concentrations south of the frontal zone remain low throughout the spring, summer, and fall. Concentrations north of the frontal zone decrease in midsummer, reducing or eliminating the frontal gradient, but increase for a brief period in early fall, reestablishing the strong frontal gradient. In the late fall, concentrations decrease north of the front, eliminating the frontal gradient, and low concentrations are again present throughout the study area.

Three principal features of interannual variability are evident in the data. In 1982 the frontal gradient is less and is displaced ≈ 150 km north of its position in other years. Also in 1982 the spring increase in concentration north of the front occurs ≈ 20 days later in the year and the fall features of the seasonal cycle occur 20–30 days earlier than previous years resulting in a “summer period” which is 40–50 days shorter than that of other years. No increase in pigment concentration takes place in the spring of 1983, and pigment concentrations throughout the transect remain low throughout this El Niño year. The frontal zone is evident for only a brief period in June.

Analysis of two-dimensional spatial patterns in the images and cross-shelf transects of the data in regions north of the front indicate that the midsummer decrease in concentration within the sampled transect is the result of changes in the cross-shelf distribution of pigment. Regions of higher pigment concentration extend 150–300 km farther offshore in spring and early summer than in mid and late summer in each year (except 1983, when higher concentrations remain closely associated with the coast throughout the year).

The time series of CZCS data is long enough to show extensive interannual variability and to identify some specific features which appear to reoccur on a regular basis.

Suggestions are made regarding mechanisms responsible for these features. Verification, however, awaits a detailed analysis of concurrent hydrographic, chemical and biological in situ measurements over seasonal time scales.

Acknowledgments. We thank those responsible for the collection and publication of the CalCOFI data, Mark Abbott for access to the CZCS West Coast Time Series, and NCAR for the meteorological data. Tim Cowles and Adriana Huyer provided helpful comments on various aspects of this work. This work was supported by NASA grant NAGW-1251 and by a Killam Postdoctoral Fellowship (A.C.T.).

REFERENCES

- Abbott, M. R., and P. M. Zion, Spatial and temporal variability of phytoplankton pigment off northern California during Coastal Ocean Dynamics Experiment 1, *J. Geophys. Res.*, *92*, 1745–1756, 1987.
- Atkinson, L. P., K. H. Brink, R. E. Davis, B. H. Jones, T. Paluszkiwicz, and D. W. Stuart, Mesoscale hydrographic variability in the vicinity of points Conception and Arguello during April–May 1983: The OPUS 1983 experiment, *J. Geophys. Res.*, *91*, 12,899–12,918, 1986.
- Brink, K. H., D. W. Stuart, and J. C. VanLeer, Observation of the coastal upwelling region near $34^\circ 30'\text{N}$ off California: Spring 1981, *J. Phys. Oceanogr.*, *14*, 378–391, 1984.
- Brinton, E., Distributional atlas of Euphausiacea (Crustacea) in the California Current region, *CalCOFI Atlas 5*, Calif. Coop. Oceanic Fish. Invest., Univ. of Calif., San Diego, La Jolla, 1967.
- Chelton, D. B., Large-scale response of the California Current to forcing by wind stress curl, *CalCOFI Rep.* *23*, pp. 130–148, Calif. Coop. Oceanic Fish. Invest., Univ. of Calif., San Diego, La Jolla, 1982.
- Chelton, D. B., Seasonal variability of alongshore geostrophic velocity off central California, *J. Geophys. Res.*, *89*, 3473–3486, 1984.
- Chelton, D. B., A. W. Bratkovitch, R. L. Bernstein, and P. M. Kosro, Poleward flow off central California during the spring and summer of 1981 and 1984, *J. Geophys. Res.*, *93*, 10,604–10,620, 1988.
- Denman, K. L., and M. R. Abbott, Time evolution of surface chlorophyll patterns from cross-spectrum analysis of satellite color images, *J. Geophys. Res.*, *93*, 6789–6798, 1988.
- Fiedler, P. C., Satellite observations of the 1982–1983 El Niño along the U.S. Pacific coast, *Science*, *224*, 1251–1254, 1984.
- Gordon, H. R., D. K. Clark, J. L. Mueller, and W. A. Hovis, Phytoplankton pigments from the Nimbus-7 coastal zone color scanner: Comparisons with surface measurements, *Science*, *210*, 63–66, 1980.
- Gordon, H. R., D. K. Clark, J. W. Brown, O. B. Brown, R. H. Evans, and W. W. Broenkow, Phytoplankton pigment concentrations in the Middle Atlantic Bight: Comparison of ship determinations and CZCS estimates, *Appl. Opt.*, *22*, 20–36, 1983.
- Hayward, T. L., and E. L. Venrick, Relation between surface chlorophyll, integrated chlorophyll and integrated primary production, *Mar. Biol.*, *69*, 247–252, 1982.
- Haurv, L. R., An offshore eddy in the California Current system, IV, Plankton distributions, *Prog. Oceanogr.*, *13*, 95–111, 1984.
- Haurv, L. R., J. J. Simpson, J. Peláez, C. J. Koblinsky, and D. Wiesenhahn, Biological consequences of a recurrent eddy off Point Conception, California, *J. Geophys. Res.*, *91*, 12,937–12,956, 1986.
- Hickey, B. M., The California Current system—Hypotheses and facts, *Prog. Oceanogr.*, *8*, 191–279, 1979.
- Husby, D. M., and C. S. Nelson, Turbulence and vertical stability in the California Current, *CalCOFI Rep.* *23*, pp. 113–129, Calif. Coop. Oceanic Fish. Invest., Univ. of Calif., San Diego, La Jolla, 1982.
- Huyer, A. E., Coastal upwelling in the California Current system, *Prog. Oceanogr.*, *12*, 259–284, 1983.
- Huyer, A. E., and R. L. Smith, The signature of El Niño off

- Oregon, 1982–1983, *J. Geophys. Res.*, *90*, 7133–7142, 1985.
- Huyer, A. E., E. J. Sobey, and R. L. Smith, The spring transition in currents over the Oregon continental shelf, *J. Geophys. Res.*, *84*, 6995–7011, 1979.
- Jones, B. H., K. H. Brink, R. C. Dugdale, D. W. Stuart, J. C. VanLeer, D. Blasco, and J. C. Kelley, Observations of a persistent upwelling center off Point Conception, California, in *Coastal Upwelling*, edited by E. Suess and J. Thiede, pp. 37–60, Plenum, New York, 1983.
- Kelly, K. A., Swirls and plumes or application of statistical methods to satellite-derived sea surface temperatures, Ph.D. thesis, *S.I.O. Ref. 83-15, CODE Tech. Rep. 18*, 210 pp., Scripps Inst. of Oceanogr., La Jolla, Calif., 1983.
- Kosro, P. M., Structure of the coastal current field off northern California during the Coastal Ocean Dynamics Experiment, *J. Geophys. Res.*, *92*, 1637–1654, 1987.
- Lynn, R. J., and J. J. Simpson, The California Current system: The seasonal variability of its physical characteristics, *J. Geophys. Res.*, *92*, 12,947–12,966, 1987.
- Lynn, R. J., K. A. Bliss, and L. E. Eber, Vertical and horizontal distributions of seasonal mean temperature, salinity, sigma- t , stability, dynamic height, oxygen, and oxygen saturation in the California Current, 1950–1978, *CalCOFI Atlas 30*, Calif. Coop. Oceanic Fish. Invest., Univ. of Calif., San Diego, La Jolla, 1982.
- McGowan, J. A., El Niño 1983 in the Southern California Bight, in *El Niño North*, edited by W. S. Wooster and D. L. Fluharty, Washington Sea Grant Program, University of Washington, Seattle, 1985.
- Mooers, C. N. K., and A. R. Robinson, Turbulent jets and eddies in the California Current and inferred cross-shore transports, *Science*, *223*, 51–53, 1984.
- Niiler, P. P., P.-M. Poulain, and L. R. Haury, Synoptic three-dimensional circulation in an onshore-flowing filament of the California Current, *Deep Sea Res.*, *36*, 385–405, 1989.
- Norton, J., D. McLain, R. Brainard, and D. Husby, The 1982–83 El Niño off Baja and Alta California and its ocean climate context, in *El Niño North*, edited by W. S. Wooster and D. L. Fluharty, Washington Sea Grant Program, University of Washington, Seattle, 1985.
- Pares-Sierra, A., and J. J. O'Brien, The seasonal and interannual variability of the California Current system: A numerical model, *J. Geophys. Res.*, *94*, 3159–3180, 1989.
- Peláez, J., and F. Guan, California Current chlorophyll measurements from satellite data, *CalCOFI Rep. 23*, pp. 212–225, Calif. Coop. Oceanic Fish. Invest., Univ. of Calif., San Diego, La Jolla, 1982.
- Peláez, J., and J. A. McGowan, Phytoplankton pigment patterns in the California Current as determined by satellite, *Limnol. Oceanogr.*, *31*, 927–950, 1986.
- Reid, J. L., Jr., R. A. Schwartzlose, and D. M. Brown, Direct measurements of a small surface eddy off northern Baja California, *J. Mar. Res.*, *21*, 205–218, 1963.
- Rienecker, M. M., and C. N. K. Mooers, The 1982–1983 El Niño signal off northern California, *J. Geophys. Res.*, *91*, 6597–6608, 1986.
- Roemmich, D., Mean transport of mass, heat, salt and nutrients in southern California coastal waters: Implications for primary production and nutrient cycling, *Deep Sea Res.*, *36*, 1359–1378, 1989.
- Roesler, C. R., and D. B. Chelton, Zooplankton variability in the California Current, 1951–1982, *CalCOFI Rep. 28*, pp. 59–96, Calif. Coop. Oceanic Fish. Invest., Univ. of Calif., San Diego, La Jolla, 1987.
- Scripps Institution of Oceanography (SIO), Physical, chemical and biological data report, *S.I.O. Ref. 84-18*, Univ. of Calif., San Diego, La Jolla, 1984a.
- Scripps Institution of Oceanography (SIO), Physical, chemical and biological data report, *S.I.O. Ref. 84-23*, Univ. of Calif., San Diego, La Jolla, 1984b.
- Scripps Institution of Oceanography (SIO), Physical, chemical and biological data report, *S.I.O. Ref. 85-9*, Univ. of Calif., San Diego, La Jolla, 1985a.
- Scripps Institution of Oceanography (SIO), Physical, chemical and biological data report, *S.I.O. Ref. 85-14*, Univ. of Calif., San Diego, La Jolla, 1985b.
- Simpson, J. J., Large-scale thermal anomalies in the California Current during the 1982–1983 El Niño, *Geophys. Res. Lett.*, *10*, 937–940, 1983.
- Simpson, J. J., El Niño-induced onshore transport in the California Current during 1982–1983, *Geophys. Res. Lett.*, *11*, 241–242, 1984a.
- Simpson, J. J., An offshore eddy in the California Current system, III, Chemical structure, *Prog. Oceanogr.*, *13*, 71–93, 1984b.
- Simpson, J. J., C. J. Koblinsky, J. Peláez, L. R. Haury, and D. Wiesenbahn, Temperature–plant pigment–optical relations in a recurrent offshore mesoscale eddy near Point Conception, California, *J. Geophys. Res.*, *91*, 12,919–12,936, 1987.
- Smith, R. C., X. Zhang, and J. Michaelson, Variability of pigment biomass in the California Current system as determined by satellite imagery, 1, Spatial variability, *J. Geophys. Res.*, *93*, 10,863–10,882, 1988.
- Strub, P. T., and C. James, Atmospheric conditions during the spring and fall transitions in the coastal ocean off western United States, *J. Geophys. Res.*, *93*, 15,561–15,584, 1988.
- Strub, P. T., J. S. Allen, A. Huyer, R. L. Smith, and R. C. Beardsley, Seasonal cycles of currents, temperatures, winds, and sea level over the northeast Pacific continental shelf: 35°N to 48°N, *J. Geophys. Res.*, *92*, 1507–1526, 1987a.
- Strub, P. T., J. S. Allen, A. Huyer, and R. L. Smith, Large-scale structure of the spring transition in the coastal ocean off western North America, *J. Geophys. Res.*, *92*, 1527–1544, 1987b.
- Strub, P. T., C. James, A. C. Thomas, and M. R. Abbott, Seasonal and nonseasonal variability of satellite-derived surface pigment concentration in the California Current, *J. Geophys. Res.*, *95*, 11,501–11,530, 1990.
- Thomas, A. C., and W. J. Emery, Relationships between near-surface plankton concentrations, hydrography, and satellite-measured sea surface temperature, *J. Geophys. Res.*, *93*, 15,733–15,748, 1988.
- Thomas, A. C., and P. T. Strub, Interannual variability in phytoplankton pigment distribution during the spring transition along the west coast of North America, *J. Geophys. Res.*, *94*, 18,095–18,117, 1989.
- Traganza, E. D., D. G. Redalje, and R. W. Garwood, Chemical flux, mixed layer entrainment and phytoplankton blooms at upwelling fronts in the California coastal zone, *Cont. Shelf Res.*, *7*, 89–105, 1987.
- Wickham, J. B., A. A. Bird, and C. N. K. Mooers, Mean and variable flow over the central California continental margin, 1978–1980, *Cont. Shelf Res.*, *7*, 827–849, 1987.
- Wyllie, J. G., Geostrophic flow of the California Current at the surface and at 20 m, *CalCOFI Atlas 4*, Calif. Coop. Oceanic Fish. Invest., Univ. of Calif., San Diego, La Jolla, 1966.

A. C. Thomas and P. T. Strub, College of Oceanography, Oregon State University, Corvallis, OR 97331.

(Received January 15, 1990;
accepted May 9, 1990.)

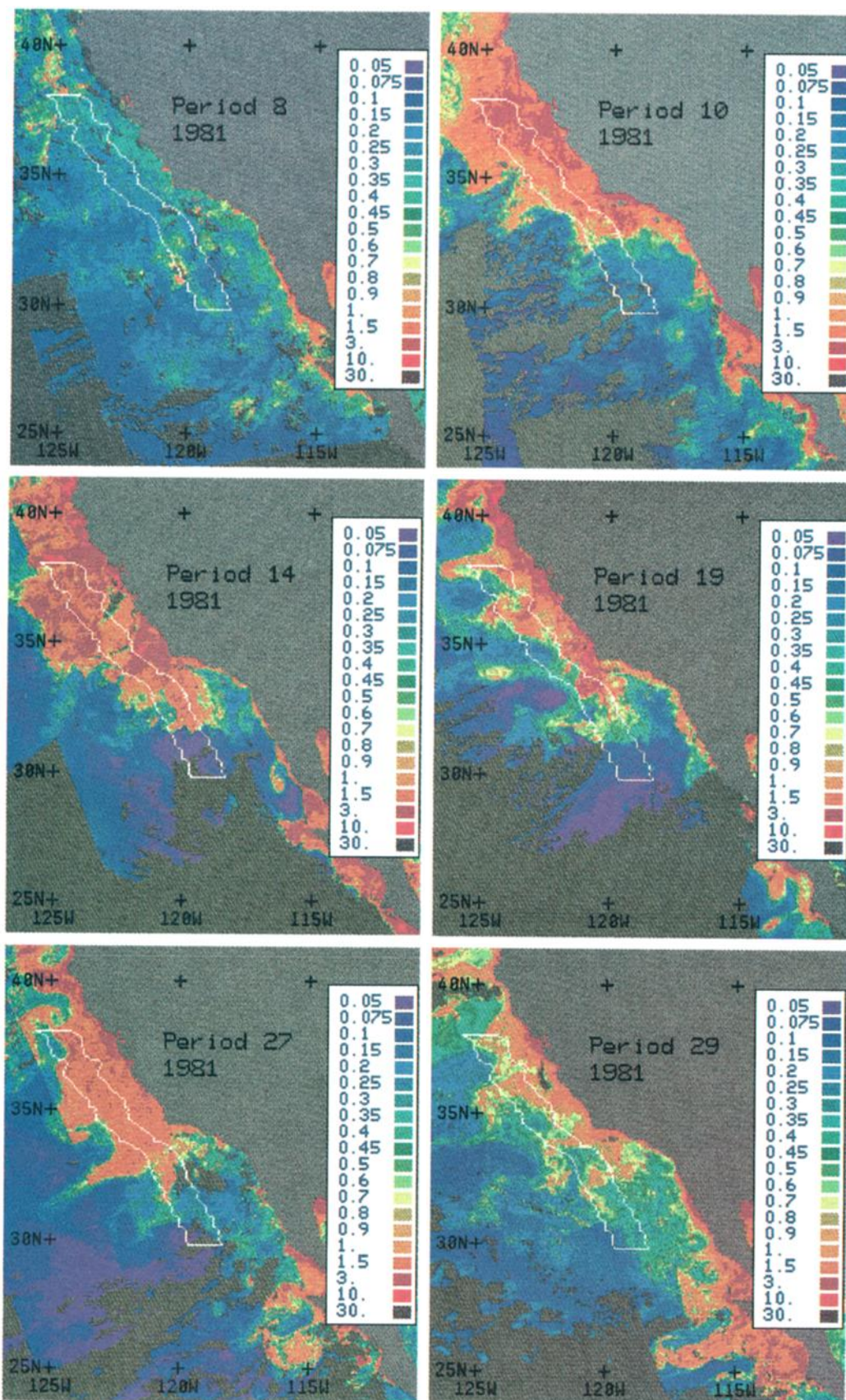


Plate 1 [Thomas and Strub]. Ten-day composite CZCS images of the periods in 1981 shown in Figure 3. Pigment concentrations are color coded as is shown in each image. Clouds, land, and missing data in each composite are masked as grey tones, and the meridional transect over which the data are zonally averaged to form a mean transect is shown.